



Ruredil **TE**chnical **DI**rection

→ **TECHNICAL NOTEBOOK**

Buildings seismic retrofit with FRCM – Fiber Reinforced Cementitious Matrix composite

Concrete and masonry structures

July 2009



INTRODUCTION

This technical notebook aims to demonstrate that Ruredil X Mesh C10 and Ruredil X Mesh Gold FRCM systems can be used for existing buildings seismic retrofit (masonry, concrete and reinforced concrete) by increasing their structural ductility.

This document is conceptually an extension specifically focusing on details of the design criteria for use of FRCM contained in the:

“Instructions for Planning Static Consolidation Projects with use of Fiber Reinforced Cementitious Matrix Compounds or FRCM”

Following design guidelines of CNR DT200-2004, this document takes a closer look at theoretical and design aspects, supported by a range of examples in application, of key projects for seismic retrofit of existing buildings, such as shear reinforcement of pillars, confinement, partition walls, etc.



TABLE OF CONTENTS

1. DELAMINATION DILATATION

2. REINFORCED CONCRETE STRUCTURES

2.1 Reinforcement work with FRCM aims

2.2 Beams and pillars shear reinforcement

2.2.1 Reinforcement Design

2.2.1.1 Examples

Example 1. Shear reinforcement of a pillar

2.3 Pillars confinement

2.3.1 Local effect: confinement of concrete

2.3.1.1 Examples

Example 1. Rectangular pillar confinement: concrete confinement

2.3.2 Effect on section: moment and bending

2.3.2.1 Examples

Example 1. Confinement of a rectangular pillar: ultimate bending and ultimate moment

2.3.3 Effect on the element: Rotation ability with reference to the chord

2.3.3.1 Examples

Example 1. Confining a rectangular pillar: Rotation ability with reference to the chord

3. MASONRY STRUCTURES

3.1 Aims of reinforcement with FRCM

3.2 Vault reinforcement

3.2.1 Reinforcement design

3.2.1.1 Examples

Example 1. Reinforcement of the extrados of a barrel vault.

Unreinforced structure

Horizontal collapse multiplier

Location of pressure centres

Acceleration of the activation of the mechanism

Reinforced structure

Horizontal multiplier of collapse

Location of the pressure centres

Acceleration of the activation of the mechanism

Stresses (moment and normal force)

Reinforcement section

Shear

4. PARTITION WALLS

4.1 Aims and criteria of reinforcement with FRCM

4.1.1 Reinforcement design

4.1.1.1 Examples

Example 1. Reinforcement against out-of-plane seismic action.



1. DELAMINATION DILATION

If we follow the instructions [1], with reference to the diagram appearing in figure 1.1, maximum delamination force of the end of an external reinforcement may be estimated as:

$$P_{dbu} = \sqrt{2p_f E_f A_f \cdot G_f} \quad (1.1)$$

corresponding to an end delamination dilatation of:

$$\varepsilon_{dbu} = \frac{P_{dbu}}{E_f A_f} = \sqrt{\frac{2p_f G_f}{E_f A_f}} \quad (1.2)$$

where:

E_f is the modulus of elasticity of the fibers;
 A_f is the area of the cross section of the fibers;
 p_f is the width of the interface surface;
 G_f is the fracture energy of the interface surface.

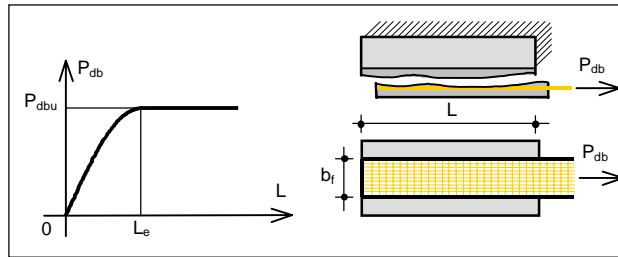


Figure 1.1. Delamination of an extremity.

Intermediate delamination dilatation may be estimated as:

$$\varepsilon_{dbm} = k_{cr} \sqrt{\frac{2p_f G_f}{E_f A_f}} \quad (1.3)$$

where k_{cr} is a coefficient to be calibrated by comparison with experimental evidence.

In the case of the Ruredil **XMesh GOLD/M750** product, in accordance with the experiments conducted (figure 1.2), we may assume:

$$p_f(n) = 2nb_f \cdot k(n) \quad k(n) = \begin{cases} 1 & \text{se } n = 1 \\ 0.8 & \text{se } 2 \leq n \leq 4 \end{cases} \quad (1.4)$$

$$G_f = 211 \frac{\text{J}}{\text{m}^2} \quad k_{cr} = 1.8 \quad (1.5)$$

in which n is the number of layers of mesh layered one on top of the other, b_f is the width of the reinforcement and $k(n)$ is an efficiency coefficient depending on the number of layers.

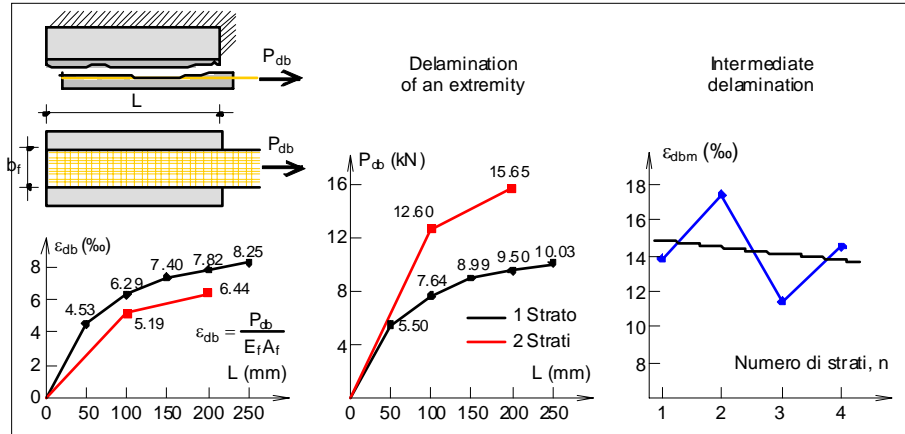


Figure 1.2. Delamination forces and dilations.

Considering the first of these (1.4) and taking into account that $A_f = n \cdot t_{1f} \cdot b_f$, (1.1) - (1.3) become:

$$P_{dbu} = 2nb_f \sqrt{k(n) \cdot E_f t_{1f} G_f} \quad \varepsilon_{dbu} = 2 \sqrt{\frac{k(n)G_f}{E_f t_{1f}}} \quad \varepsilon_{dbm} = 2k_{cr} \sqrt{\frac{k(n)G_f}{E_f t_{1f}}} \quad (1.6)$$

where $t_{1f} = 0.046$ mm is the thickness of a single layer of mesh (“strong” direction).

Use of (1.6) in the plan requires adoption of the “calculation” properties of the materials:

$$P_{fde} = \frac{2nb_f}{\gamma_{Rd}} \sqrt{k(n) \cdot E_f t_{1f} G_{fd}} \quad \varepsilon_{fde} = \frac{2}{\gamma_{Rd}} \sqrt{\frac{k(n)G_{fd}}{E_f t_{1f}}} \quad \varepsilon_{fdm} = \frac{2k_{cr}}{\gamma_{Rd}} \sqrt{\frac{k(n)G_{fd}}{E_f t_{1f}}} \quad (1.7)$$

where:

γ_{Rd} is the partial coefficient of the adherence model (to be assumed to be 1.2);
 G_{fd} is the calculated fracture energy of the interface surface:

$$G_{fd} = \frac{G_{fd}}{\gamma_g} \quad (1.8)$$

where γ_g is the partial safety coefficient (values between 1.3 and 1.6 are suggested).

Note that the limits (1.6) on delamination of extremities and the corresponding calculated values (1.7) refer to a fiber anchorage length greater than effective transfer length, L_e (figure 1.1). For the product under consideration this length is about 250 mm (figure 1.2).

Moreover, the limits (1.6) and the corresponding calculation values (1.7) have been estimated on the basis of the results of experiments with specimens consisting of good quality concrete ($R_{ck} > 35$ MPa). In the event of application on poor quality concrete, these limits must be reduced appropriately.

2. REINFORCED CONCRETE STRUCTURES

2.1 Aims of reinforcement work with FRCM

Reinforcement of structures with a reinforced concrete frame with FRCM materials in seismic zones is particularly useful for achieving the following aims.

- i) Increasing resistance to shearing stress of beams and pillars to create the correct hierarchy of resistances between fragile mechanisms and ductile mechanisms.
- ii) Increasing the ductility of the terminal parts of beams and pillars which are likely to contain plastic hinges.
- iii) Improving anchorage of longitudinal bars in overlapping areas.
- iv) Creating an obstacle to warping of longitudinal bars in pillars.
- v) Increasing the strength of nodes.



These aims fit into the context of the more goal of increasing seismic capacity by increasing structural ductility. Structural ductility, by which we mean the capacity of structures to be deformed well beyond the elastic limit on materials, is in fact an essential requirement for the survival of structures subject to seismic action, as recognised by the most recent standards and instructions.

Some of the aims listed above result in an increase in the collapse loads associated with fragile mechanisms (cutting, local node breakage, withdrawal of reinforcement bars, compression of concrete), making them superior to the collapse loads associated with ductile mechanisms (bending with abundantly yielded reinforcement).

The other aims, on the other hand, increase local ductility at the points corresponding to parts of the structure which, upon collapse, reach the limits on resistance (plastic hinges).

Achievement of these aims therefore promotes structural collapse due to formation of plastic hinges and increases their deformational capacity.

2.2 Reinforcing shear strength of beams and pillars

The shear strength of a reinforced concrete structure may be improved by applying FRCM composite materials to its side surfaces, with the fibers lying across the longitudinal axis (figure 2.1). The most frequent case is definitely that in which fibers lie at right angles to the axis of the element (figure 2.2).

2.2.1 Design of the reinforcement

According to the approach described in the guidelines [1], the shear strength of a concrete element reinforced with composite materials may be estimated as follows:

$$V_{Rd} = \min\{V_{Rdct} + V_{Rds} + V_{Rdf}; V_{Rdmax}\} \quad (2.1)$$

where V_{Rdct} and V_{Rds} are the contributions to resistance associated with the concrete and the cross steel reinforcements, V_{Rdmax} is the resistance associated with breakage of the connecting rods in the compressed concrete wall and V_{Rdf} is the contribution to resistance associated with reinforcement with composite material. The quantities V_{Rdct} and V_{Rds} are estimated as usual in the case of unreinforced elements.

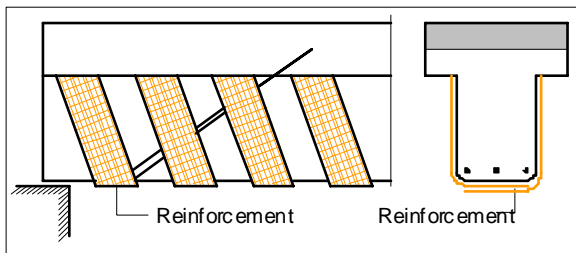


Figure 2.1. Reinforcement of a girder's shear strength.

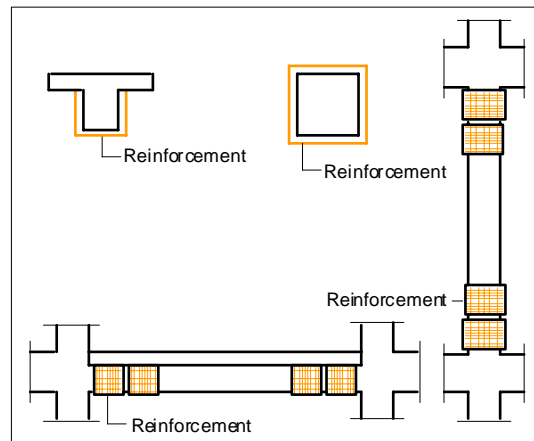


Figure 2.2. Reinforcement of a girder and a pillar.

The contribution associated with fiber reinforcement is created by:

$$V_{Rdf} = \frac{1}{\gamma_{Rdv}} \cdot 0.9 \cdot d \cdot \frac{2t_f w_f}{i_f} \cdot E_f \cdot \varepsilon_{fdv} (\cot \theta + \cot \beta) \cdot \sin \beta \quad (2.2)$$

where (figure 2.3):

- γ_{Rdv} is the partial coefficient of the resistance model (assumed to be equal to 1.2);
- d is the useful height of the section;
- w_f is the width of each band of reinforcement;
- i_f is the centre-to-centre distance between bands of reinforcement;
- E_f is the modulus of elasticity of the reinforcement;
- ε_{fdv} is the calculated dilatation of reinforcement of shear strength (linked with dilatation of the ends);
- θ is the inclination of compressed concrete connecting rods in relation to the element's axis;



β is the inclination of the reinforcement fibers in relation to the element's axis.

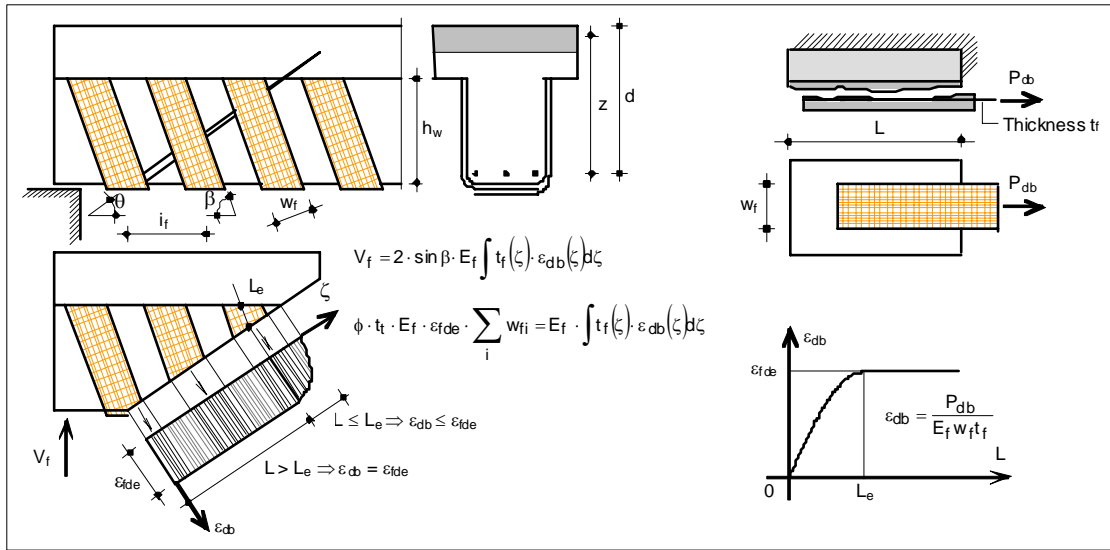


Figure 2.3. Calculation diagram for reinforcement of shear strength.

(2.2) follows directly from the Mörsh's trellis approach and may be applied to reinforcement with FRCM materials, once calculation dilation ε_{fdv} and effective transfer length L_e have been defined.

Calculated dilation of reinforcement of shear strength is equal to the average dilation of the fibers that cross an ideal crack due to shear stress, under the conditions of delamination of the reinforcement.

In the case of FRCM reinforcements arranged in a U shape around the core of the beam (figure 2.3), we must take into account the fact that not all the fibers crossing a generic cut caused by shear stress are anchored by more than L_e . And so, upon delamination of the reinforcement, not all the fibers can reach the dilatation of delamination of the extremity ε_{fde} . In this case dilation ε_{fdv} is determined by dilation of delamination of the reinforcement fibers, as shown in figure 2.3. This is the same as introducing an "efficiency" coefficient ϕ defined as:

$$\phi = 1 - \frac{1}{3} \cdot \frac{L_e}{h_w} \cdot \sin \beta \quad (2.3)$$

and determining calculated dilation of the reinforcement of shear strength as:

$$\varepsilon_{fdv} = \phi \cdot \varepsilon_{fde} \quad (2.4)$$

In the case of pillars reinforced with FRCM (figure 2.2), the fibers wrap around the entire section, and we may suppose that they are all anchored by more than L_e . And so it seems reasonable to assume:

$$\varepsilon_{fdv} = \varepsilon_{fde} \quad (2.5)$$

In the frequent case of U-shaped reinforcement with FRCM arranged continuously with the fibers at right angles to the element's axis, (2.2) and (2.3) become:

$$V_{Rdf} = \frac{0.9 \cdot d}{\gamma_{Rdv}} \cdot 2t_f \cdot E_f \cdot \varepsilon_{fdv} = \quad (2.6)$$

$$\phi = 1 - \frac{1}{3} \cdot \frac{L_e}{h_w} \quad (2.7)$$

2.2.1.1 Examples

Example 1. Shear reinforcement of a pillar (Resistance Hierarchy).

Let us consider a pillar with a section measuring $300 \times 400 \text{ mm}^2$, a height of $l_p = 3 \text{ m}$, consisting of concrete with $f_{ck} = 20 \text{ MPa}$ and the reinforcements shown in figure 2.4, made of Feb44k steel.

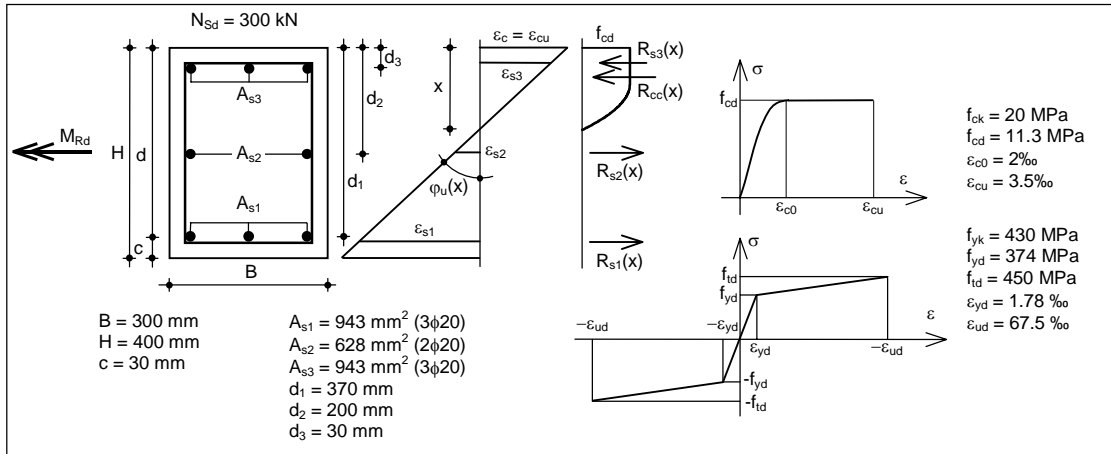


Figure 2.4. Pillar: section and materials.

If we want to determine the scale of reinforcement of shear strength with XMesh GOLD/M750 so as to satisfy the ratio of the Resistance Hierarchy:

$$V_{Rd} \geq V_{Ed} = \gamma_{Rd} \frac{|M_{Rd}^S + M_{Rd}^I|}{l_p}$$

where:

V_{Rd} is the calculated shear strength;

V_{Ed} is the shear stress used in calculation, in accordance with the Resistances Hierarchy;

M_{Rd}^S is the moment of resistance of the top section;

M_{Rd}^I is the moment of resistance of the bottom section;

γ_{Rd} is the over-resistance coefficient, assumed to be equal to 1.1 (CD B).

Combined compressive and bending stress calculation at the end sections of the pillar gives us the resistance domain (M_{Rd} , N_{Rd}) shown in figure 2.5.

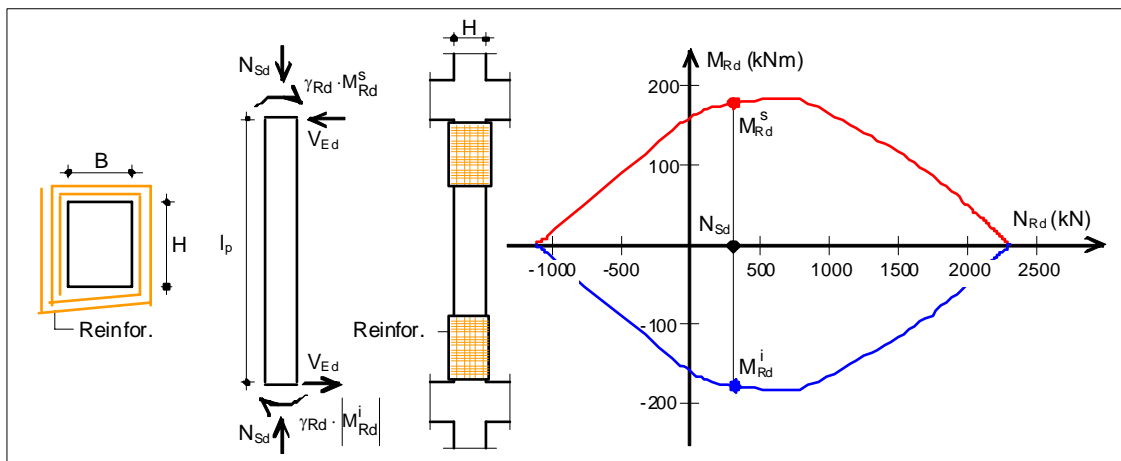


Figure 2.5. Reinforcement configuration.

Considering a normal acting force of $N_{Sd} = 300 \text{ kN}$, under breakage conditions (figures 2.4 and 2.5), we obtain:

| | |
|--------------------------------|---|
| $x = 156.4 \text{ mm}$ | distance of the neutral axis from the compressed edge |
| $\epsilon_c = 3.5\text{‰}$ | maximum concrete deformation |
| $\epsilon_{s1} = 4.77\text{‰}$ | deformation of reinforcement on three levels |
| $\epsilon_{s2} = 0.97\text{‰}$ | |



$$\varepsilon_{s3} = 2.83 \text{ ‰}$$

$$M_{Rd} = 178.7 \text{ kNm} \quad \text{calculated moment of resistance}$$

And so the acting shear stress in accordance with the Resistance Hierarchy will be:

$$V_{Ed} = \gamma_{Rd} \frac{|M_{Rd}^s| + |M_{Rd}^i|}{l_p} = 1.1 \frac{178.7 + 178.7}{3} = 131.05 \text{ kN}$$

If we neglect the concrete's contribution and consider $\theta = 45^\circ$ (inclination of compressed connecting rods), the calculated shear strength will be:

$$V_{Rd0} = V_{Rds} = 0.9 \cdot d \cdot \frac{A_{sw}}{i_s} \cdot f_{yd} = 0.9 \cdot 0.37 \cdot \frac{1.005 \cdot 10^{-4}}{0.2} \cdot 3.74 \cdot 10^5 = 62.58 \text{ kN}$$

Considering that the pillar is wrapped in two layers of XMesh GOLD reinforcement (figure 2.5), the contribution the reinforcement gives to shear strength is:

$$V_{Rdf} = \frac{0.9 \cdot d}{\gamma_{Rdv}} \cdot 2t_f \cdot E_f \cdot \varepsilon_{fdv} = \frac{0.9 \cdot 370}{1.2} \cdot 2 \cdot 0.09 \cdot \frac{270000}{1000} \cdot \frac{5.3}{1000} = 71.48 \text{ kN}$$

as

$$t_f = 2 \cdot t_{1f} = 0.09 \text{ mm}$$

where $t_{1f} = 0.045 \text{ mm}$ is the nominal thickness of the individual layer of reinforcement, and having assumed, in accordance with (1.7) and (1.8):

$$\varepsilon_{fde} = \frac{2}{\gamma_{Rd}} \sqrt{\frac{k(n)G_{fd}}{E_f t_{1f}}} = \frac{2}{1.2} \sqrt{\frac{0.8 \cdot 0.156}{270000 \cdot 0.045}} = 5.3 \text{ ‰} \quad G_{fd} = \frac{G_f}{\gamma_g} = \frac{211}{1.35} = 156 \frac{\text{J}}{\text{m}^2}$$

where $k(2) = 0.8$, $\gamma_{Rd} = 1.2$, $G_f = 211 \text{ J/m}^2$, $\gamma_g = 1.35$.

Shear strength with reinforcement is therefore:

$$V_{Rd} = V_{Rds} + V_{Rdf} = 62.58 + 71.48 = 134.07 \text{ kN} > V_{Ed} = 131.05 \text{ kN}$$

Note that the estimates above were made in a simplified, precautionary manner, without taking into account the effect of reinforcement confining, discussed in the next section.

2.3 Confining pillars

Confinement of a pillar with FRCM composite material is achieved by winding the composite material around the drum of the pillar (figure 2.6). The effects of this reinforcement configuration are:

- increase in shear strength (as discussed in the previous point);
- increase of deformation capability of the compressed concrete;
- increase in the concrete's compression strength.

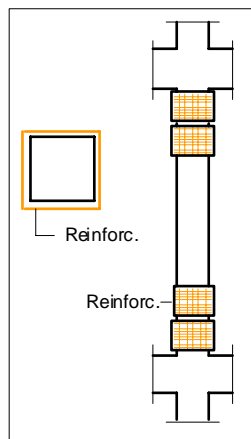


Figure 2.6. Confinement of the ends of a pillar.



2.3.1 Local effect: confinement of concrete

Confining with composite material produces an obstacle to the transverse dilatation of concrete associated with normal compression force and therefore an increase in the concrete's resistance and ultimate deformation under compression. Having determined these increases, we may make structural assessments considering the binding link of the confined concrete.

According to the approach set forth in the guidelines [1], the confined concrete's calculated compression strength f_{ccd} and ultimate deformation under compression ε_{ccu} are:

$$f_{ccd} = f_{cd} \cdot \left[1 + 2.6 \cdot \left(\frac{f_{Leff}}{f_{cd}} \right)^{\frac{2}{3}} \right] \quad (2.8)$$

$$\varepsilon_{ccu} = 0.0035 + 0.015 \cdot \sqrt{\frac{f_{Leff}}{f_{cd}}} \quad (2.9)$$

where:

f_{cd} is the calculated compression strength of the unconfined concrete;
 f_{Leff} is the effective confining pressure produced by the reinforcement.

Effective confining pressure f_{Leff} is the product of an efficiency coefficient k_{eff} which depends on geometry to determine encircling pressure f_L :

$$f_{Leff} = k_{eff} \cdot f_L \quad (2.10)$$

Confining pressure f_L (figure 7) may be calculated as:

$$f_L = \frac{1}{2} \rho_f E_f \cdot \varepsilon_{fdc} \quad (2.11)$$

where ε_{fdc} is the calculated actual dilation of the confining reinforcement, while the geometric reinforcement percentage is:

$$\rho_f = \frac{4t_f \cdot b_f}{D \cdot i_f} \quad \text{for circular sections of diameter } D \quad (2.12)$$

$$\rho_f = \frac{2t_f \cdot (B+H) \cdot b_f}{B \cdot H \cdot i_f} \quad \text{for rectangular sections with dimensions } B \text{ and } H$$

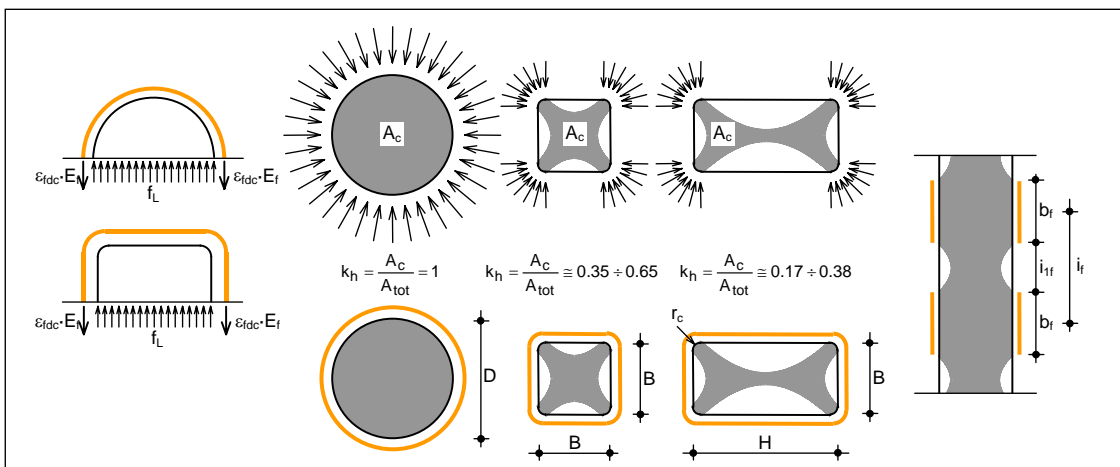


Figure 2.7. Confinement of pillars.

The efficiency coefficient depends on the shape of the section and the geometry of the reinforcement and is calculated as follows:



$$k_{\text{eff}} = k_h \cdot k_v \cdot k_\alpha \quad (2.13)$$

where k_h takes into account the shape of the section and is the ratio between the effectively circled concrete section A_c , the total section A_{tot} , k_v takes into account the distribution of reinforcements along the axis of the pillar and k_α takes into account the inclination α of the fibers (figure 2.7):

$$k_h = \frac{A_c}{A_{\text{tot}}} \quad k_v = \left(1 - \frac{i_{\text{ff}}}{2 \cdot d_{\text{min}}}\right)^2 \quad k_\alpha = \frac{1}{1 + \tan^2 \alpha} \quad (2.14)$$

as d_{min} is the minimum crosswise dimension of the element (diameter D in circular sections), and i_{ff} the extension of the unreinforced area between two consecutive strips, measured along the axis of the element. In the case of pillars with a rectangular section with corners rounded off and a rounding radius of r_c , the first of (2.7) becomes:

$$k_h = 1 - \frac{(B - 2r_c)^2 + (H - 2r_c)^2}{3 \cdot A_g} \quad (2.15)$$

where A_g is the area of the cross section (not including rounded off corners).

The guidelines [1] suggest, in the case of assessment of resistance to simple compression of the confined pillar, that we assume:

$$\varepsilon_{\text{fdc}} = 4\text{‰} \quad (2.16)$$

and, for calculating resistance to flex fatigue and ductility, that we assume:

$$\varepsilon_{\text{fdc}} = 0.6 \cdot \varepsilon_{\text{fk}} \quad (2.17)$$

where ε_{fk} is the reinforcement's characteristic breakage dilatation.

In the case of FRCM XMesh GOLD/M750 reinforcement, taking into account crisis caused by delamination, in the second case it is reasonable to assume:

$$\varepsilon_{\text{fdc}} = \varepsilon_{\text{fde}} \quad (2.18)$$

2.3.1.1 Examples

Example 1. Confining a rectangular pillar: confined concrete.

If we consider a pillar with a rectangular section measuring 30 x 40 cm² consisting of concrete with a characteristic resistance to cylindrical compression of $f_{\text{ck}} = 20$ MPa, and suppose that we adopt a corner curve radius of $r_c = 30$ mm (figure 2.8) and encircle the section with two continuous layers of XMesh GOLD reinforcement, laying the fibers horizontally (the mesh's strong direction) and vertically, the unconfined concrete's calculated compression strength, according to [2], will be:

$$f_{\text{cd}} = \frac{\alpha_c}{\gamma_c} \cdot f_{\text{ck}} = \frac{0.85}{1.5} \cdot 20 = 11.3 \text{ MPa}$$

The geometric reinforcement percentage is:

$$\rho_f = \frac{2t_f \cdot (B + H)}{B \cdot H} \cdot \frac{b_f}{i_f} = \frac{2 \cdot 0.09 \cdot (300 + 400)}{300 \cdot 400} = 1.05\text{‰}$$

where $t_f = 0.09$ mm (double layer) and $b_f/i_f = 1$ (continuous wrapping along the axis). The efficiency coefficients are:

$$k_h = 1 - \frac{(B - 2r_c)^2 + (H - 2r_c)^2}{3 \cdot A_g} = 1 - \frac{(300 - 60)^2 + (400 - 60)^2}{3 \cdot \left[300 \cdot 400 - \left(1 - \frac{\pi}{4}\right) \cdot 30^2\right]} = 0.516$$

$$k_v = \left(1 - \frac{i_{\text{ff}}}{2 \cdot d_{\text{min}}}\right)^2 = 1$$



$$k_{\alpha} = \frac{1}{1 + \tan^2 \alpha} = 1$$

as in this case $\alpha = 0$ and $i_{rf} = 0$.
Confining pressure will be:

$$f_L = \frac{1}{2} \rho_f E_f \cdot \varepsilon_{fdc} = \frac{1}{2} \cdot \frac{1.05}{1000} \cdot 270000 \cdot \frac{5.3}{1000} = 0.751 \text{ MPa}$$

and effective confining pressure will be:

$$f_{Leff} = k_{eff} \cdot f_L = k_h \cdot k_v \cdot k_{\alpha} \cdot f_L = 0.751 \cdot 1 \cdot 1 \cdot 0.516 = 0.387 \text{ MPa}$$

The calculated compression strength and ultimate deformation of the confined concrete will therefore be:

$$f_{ccd} = f_{cd} \cdot \left[1 + 2.6 \cdot \left(\frac{f_{Leff}}{f_{cd}} \right)^{\frac{2}{3}} \right] = 11.3 \cdot \left[1 + 2.6 \cdot \left(\frac{0.387}{11.3} \right)^{\frac{2}{3}} \right] = 11.3 \cdot 1.275 = 14.4 \text{ MPa}$$

$$\varepsilon_{ccu} = 0.0035 + 0.015 \cdot \sqrt{\frac{f_{Leff}}{f_{cd}}} = 0.0035 + 0.015 \cdot \sqrt{\frac{0.387}{11.3}} = 6.27 \text{ ‰}$$

As we can see, confining has a much greater impact on ultimate deformation (a 79.2% increase) than on strength (a 27.4% increase).

Appendix D to the guideline [1] also suggests that when modelling the mechanical behaviour of confined elements we should adopt a constitutive relation consisting of an initial parabolic section, up to 2‰ deformation, and a second section at a constant slope up to a deformation of ε_{ccu} (figure 2.9).

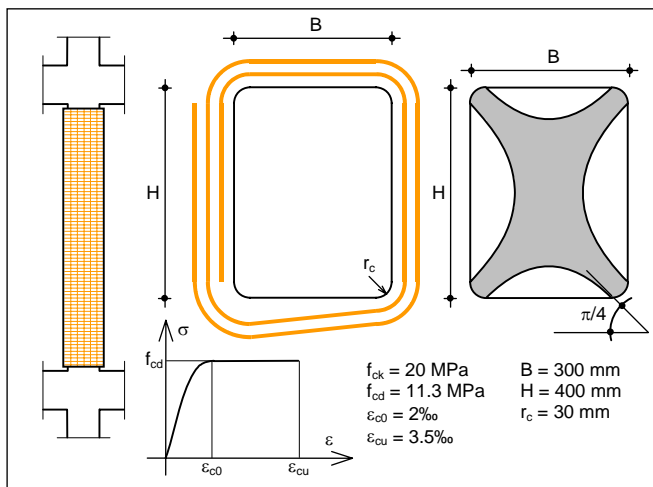


Figure 2.8. Reinforcement configuration.

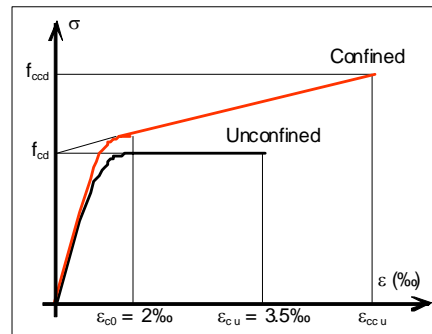


Figure 2.9. Link constituting confined and unconfined concrete.

In the case under consideration, if we apply the procedure illustrated, we obtain the constitutive relations shown in figure 2.10, pertaining to adoption of a number of layers of reinforcement, corresponding to the ultimate strengths and deformations shown in table 2.1.

| | Compression strength, f_{ccd} (MPa) | f_{ccd}/f_{cd} | Ultimate deformation ε_{ccu} (‰) | $\varepsilon_{ccu}/\varepsilon_{cu}$ |
|--------------|--|------------------|---|--------------------------------------|
| Unreinforced | 11.3 | -- | 3.50 | -- |
| 1 layer | 13.3 | 1.17 | 5.46 | 1.56 |
| 2 layers | 14.4 | 1.27 | 6.27 | 1.79 |
| 3 layers | 15.4 | 1.36 | 6.90 | 1.97 |
| 4 layers | 16.3 | 1.43 | 7.42 | 2.12 |

Table 2.1. Effect of confining on the concrete's behaviour under compression. f_{cd} : calculated compression strength without reinforcement; ε_{cu} : ultimate deformation without reinforcement.

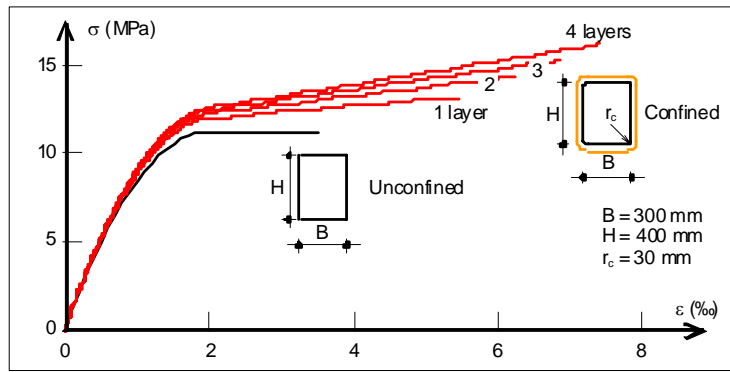


Figure 2.10. Constitutive relation in concrete with different degrees of confining.

2.3.2 Sectional effect: moment and bending

The constitutive relations in figure 2.10 may be used in a conservation model of flat sections (figure 2.11) for determination of calculated moment of resistance and ultimate bending of the section.

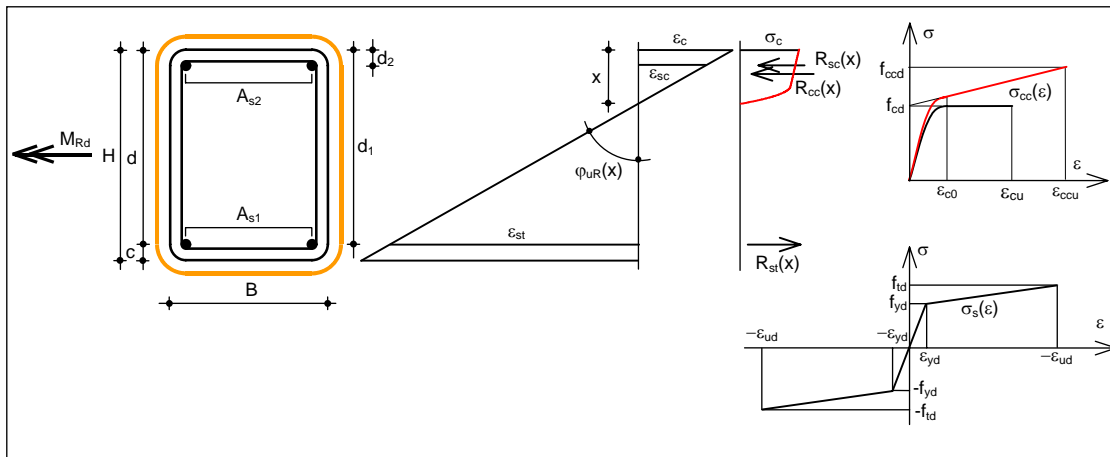


Figure 2.11. Diagram for determination of ultimate moment and ultimate bending.

The ultimate bending of the confined section is:

$$\varphi_{UR}(x) = \frac{\epsilon_{ud}}{d-x} \quad \text{in the case of breakage due to reaching the steel's ultimate deformation point} \quad (2.19)$$

$$\varphi_{UR}(x) = \frac{\epsilon_{ccu}}{x} \quad \text{in the case of breakage due to ultimate deformation of confined concrete}$$

where the distance x of the neutral axis of the compressed edge is the solution to the equilibrium equation:

$$R_{cc}(x) + R_{sc}(x) - R_{st}(x) = N_{Sd} \quad (2.20)$$

as $R_{cc}(x)$, $R_{sc}(x)$, $R_{st}(x)$ and N_{Sd} are, respectively, the result of compression tensions in the concrete, the results of compression and the results of tensile stress in the steel and the normal calculated acting force. These results may be calculated as follows:

$$\begin{aligned} R_{sc}(x) &= A_{s2} \cdot \sigma_s(\varphi_{UR}(x)) \cdot (x - c) & R_{st}(x) &= A_{s1} \cdot \sigma_s(\varphi_{UR}(x)) \cdot (d - x) \\ R_{cc}(x) &= B \cdot \int_0^x \sigma_{cc}(\varphi_{UR}(x) \cdot z) dz \end{aligned} \quad (2.21)$$

where $\sigma_{cc}(\epsilon)$ and $\sigma_s(\epsilon)$ are the constitutive relations of confined concrete and steel (figure 11). The calculated moment of resistance of the confined section is given by the equilibrium equation:



$$M_{Rd} = B \cdot \int_0^x \sigma_{cc}(\varphi_{uR}(x) \cdot z) \cdot \left(\frac{H}{2} - x + z\right) dz + A_{s2} \cdot \sigma_s(\varphi_{uR}(x) \cdot (x - c)) \cdot \left(\frac{H}{2} - c\right) + A_{s1} \cdot \sigma_s(\varphi_{uR}(x) \cdot (d - x)) \cdot \left(d - \frac{H}{2}\right) \quad (2.22)$$

2.3.2.1 Examples

Example 1. Confining a rectangular pillar: ultimate bending and ultimate moment.

If we once again consider the pillar taken in the previous example, if it is confined with two layers of XMesh GOLD we have the constitutive relation in the confined concrete shown in figure 2.10. Considering $N_{sd} = 350$ kN and the reinforcements shown in figure 2.12, the solution to the equilibrium equation (2.20) gives us:

$$x = 101.5 \text{ mm}$$

which corresponds to the crisis due to reaching the encircled concrete's ultimate deformation point, and therefore ultimate curve:

$$\varphi_{uR}(x) = \frac{\varepsilon_{ccu}}{x} = \frac{6.28}{1000 \cdot 0.1014} = 0.062 \frac{1}{m}$$

Upon breakage the materials' deformation points are as follows:

$$\varepsilon_{cmax} = \varepsilon_{ccu} = \varphi_{uR}(x) \cdot x = 0.062 \cdot 0.1014 = 6.28 \text{ ‰}$$

$$\varepsilon_{s1} = \varphi_{uR}(x) \cdot (d - x) = 0.062 \cdot (0.37 - 0.1014) = 16.63 \text{ ‰}$$

$$\varepsilon_{s2} = \varphi_{uR}(x) \cdot (x - c) = 0.062 \cdot (0.1014 - 0.03) = 4.22 \text{ ‰}$$

The results of tensile stress and compression are:

$$R_{cc}(x) = B \cdot \int_0^x \sigma_{cc}(\varphi_{uR}(x) \cdot z) dz = 0.3 \cdot \int_0^{0.1015} \sigma_{cc}(0.062 \cdot z) dz = 355.6 \text{ kN}$$

$$R_{sc}(x) = A_{s2} \cdot \sigma_s(\varphi_{uR}(x) \cdot (x - c)) = 402 \cdot \sigma_s\left(\frac{4.22}{1000}\right) = 151.6 \text{ kN}$$

$$R_{st}(x) = A_{s1} \cdot \sigma_s(\varphi_{uR}(x) \cdot (d - x)) = 402 \cdot \sigma_s\left(\frac{16.63}{1000}\right) = 157.2 \text{ kN}$$

Lastly, by applying (2.22), we may obtain calculated moment of resistance:

$$M_{Rd} = 107.9 \text{ kNm}$$

If we repeat the calculation for unconfined concrete (figure 2.12), that is, repeating the formulas above with the constitutive relation of unconfined concrete in place of that of confined concrete, we have:

$$x = 127.8 \text{ mm} \quad \varphi_u(x) = \frac{\varepsilon_{cu}}{x} = \frac{3.5}{1000 \cdot 0.1278} = 0.027 \frac{1}{m}$$

$$\varepsilon_{cmax} = \varphi_u(x) \cdot x = 0.027 \cdot 0.1278 = 3.5 \text{ ‰}$$

$$\varepsilon_{s1} = \varphi_u(x) \cdot (d - x) = 0.027 \cdot (0.37 - 0.1278) = 6.63 \text{ ‰}$$

$$\varepsilon_{s2} = \varphi_{uR}(x) \cdot (x - c) = 0.027 \cdot (0.1278 - 0.03) = 2.68 \text{ ‰}$$

$$M_{Rd} = 103.2 \text{ kNm}$$

Comparison of the breakage point of the confined section and the unconfined section is shown in figure 2.12. As we may see, in terms of sections too, the effect of confining is much greater when it comes to ultimate deformation (a 126% increase) than resistance (a 4.5% increase).

Table 2.2 shows the moments and ultimate bendings determined for the section under consideration as described above, for different layers of reinforcement.



| | M_{Rd} (kNm) | M_{Rd}/M_{Rd0} | φ_{uR} (1/m) | $\varphi_{uR}/\varphi_{uR0}$ |
|--------------|-------------------|------------------|-------------------------|------------------------------|
| Unreinforced | 103.3 | -- | 0.027 | -- |
| 1 layer | 106.4 | 1.03 | 0.051 | 1.85 |
| 2 layers | 107.9 | 1.05 | 0.062 | 2.26 |
| 3 layers | 109.1 | 1.06 | 0.071 | 2.60 |
| 4 layers | 110.0 | 1.07 | 0.080 | 2.91 |

Table 2.2. Calculated moment of resistance and ultimate bending. M_{Rd0} : calculated moment of resistance without reinforcement (corresponding to N_{Sd}); φ_{uR0} : ultimate bending without reinforcement.

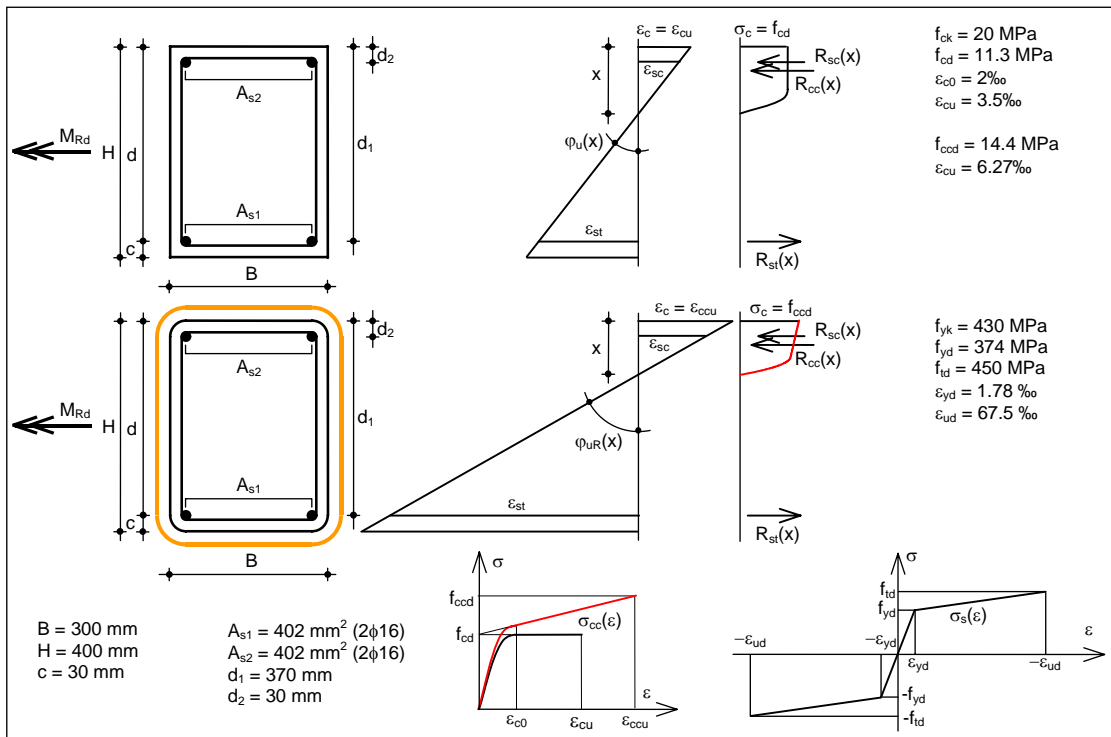


Figure 2.12. Comparison of confined section and unconfined section at the breakage point.

If we repeat the calculation for different values of normal acting force, we obtain the resistance domains (M_{Rd} , N_{Rd}) for the reinforced section shown in figure 2.13.

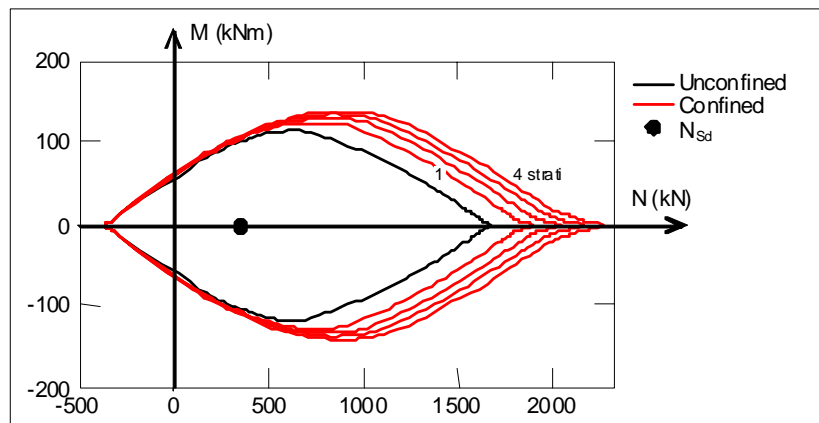


Figure 2.13. Resistance domains upon variation of the degree of confining.



2.3.3 Effect on the element: capacity for rotation with respect to the chord

The increase in the section's capacity for deformation produces an increase in the structure's overall capacity for deformation. This increased capacity may be calculated on the basis of capacity for rotation with respect to a chord, defined as the ratio between transverse shift of a section with a moment of null and the shear span L_v (figure 2.14).

According to [1], rotation capacity with respect to the chord of the confined pillar may be calculated as follows:

$$\theta_u = \frac{1}{\gamma_{el}} \cdot \left[\theta_y + (\varphi_u - \varphi_y) \cdot \left(1 - \frac{L_{pl}}{2L_v} \right) \cdot L_{pl} \right] \quad (2.23)$$

where:

- γ_{el} is a factor equal to 1.5 for the main structural elements and 1.0 for the secondary ones;
- θ_y is rotation with respect to the chord upon yielding of tense longitudinal bars;
- φ_u the section's ultimate bending;
- φ_y the section's curve when the steel bars yield;
- L_{pl} the length of the plastic hinge;
- L_v the shear span.

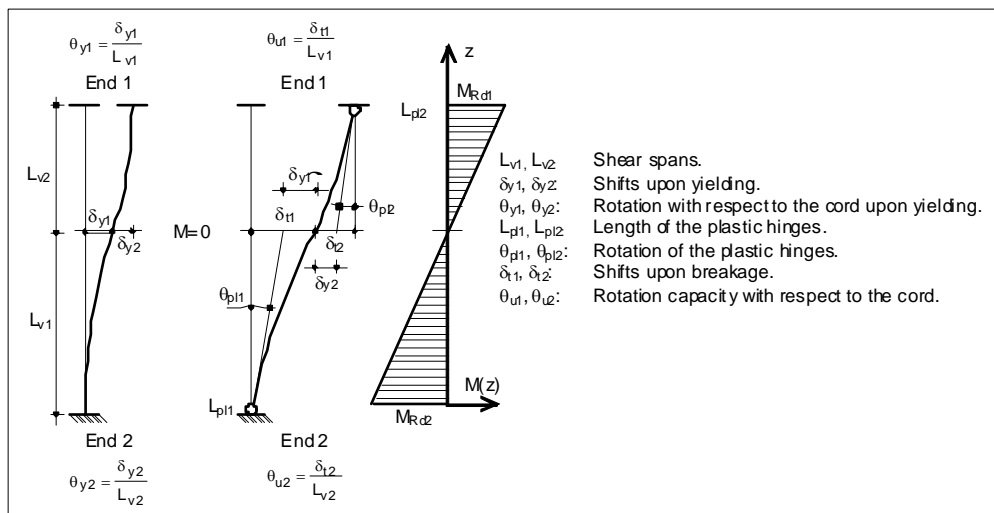


Figure 2.14. Rotation with respect to the chord.

Also in accordance with [1], rotation with respect to the chord upon yielding of tense longitudinal bars, θ_y , and the length of the plastic hinge L_p may be calculated as follows:

$$\theta_y = \varphi_y \cdot \frac{L_v}{3} + 0.0013 \cdot \left(1 + 1.5 \cdot \frac{H}{L_v} \right) + 0.13 \cdot \varphi_y \cdot \frac{d_b f_y}{\sqrt{f_c}} \quad (2.24)$$

$$L_{pl} = 0.1 \cdot L_v + 0.17 \cdot H + 0.24 \cdot \frac{d_b f_y}{\sqrt{f_c}} \quad (2.25)$$

where:

- d_b is the average diameter of the longitudinal bars;
- f_y is the yield tension of the longitudinal bars;
- f_c is the concrete's compression strength.



2.3.3.1 Examples

Example 1. Confining a rectangular pillar: capacity for rotation with respect to the chord.

Once again considering the pillar in the previous example, in the case of confinement with two layers of XMesh GOLD we have:

$$L_{pl} = 0.1 \cdot L_v + 0.17 \cdot H + 0.24 \cdot \frac{d_b f_y}{\sqrt{f_c}} = 0.1 \cdot 1.5 + 0.17 \cdot 0.4 + 0.24 \cdot \frac{0.016 \cdot 374}{\sqrt{14.4}} = 0.60 \text{ m}$$

$$\begin{aligned} \theta_y &= \varphi_y \cdot \frac{L_v}{3} + 0.0013 \cdot \left(1 + 1.5 \cdot \frac{H}{L_v}\right) + 0.13 \cdot \varphi_y \cdot \frac{d_b f_y}{\sqrt{f_c}} = \\ &= 0.0093 \cdot \frac{1.5}{3} + 0.0013 \cdot \left(1 + 1.5 \cdot \frac{0.4}{1.5}\right) + 0.13 \cdot 0.0093 \cdot \frac{0.016 \cdot 374}{\sqrt{14.4}} = 8.36 \cdot 10^{-3} = 0.48^\circ \end{aligned}$$

where bending and bending moment upon yielding of the tense steel bars are:

$$\varphi_y = 0.0093 \frac{1}{\text{m}} \qquad M_y = 97.29 \text{ kNm}$$

and considering the shear span L_v to be 1.5 m.

Rotation capacity with respect to the chord will therefore be:

$$\begin{aligned} \theta_u &= \frac{1}{\gamma_{el}} \cdot \left[\theta_y + (\varphi_u - \varphi_y) \cdot \left(1 - \frac{L_{pl}}{2L_v}\right) \cdot L_{pl} \right] = \\ &= \frac{1}{1.5} \cdot \left[8.36 \cdot 10^{-3} + (0.062 - 0.0093) \cdot \left(1 - \frac{0.6}{2 \cdot 1.5}\right) \cdot 0.6 \right] = 0.022 = 1.28^\circ \end{aligned}$$

if we consider $\gamma_{el} = 1.5$.

The same quantities for the unconfined section are:

$$L_{pl} = 0.1 \cdot L_v + 0.17 \cdot H + 0.24 \cdot \frac{d_b f_y}{\sqrt{f_c}} = 0.1 \cdot 1.5 + 0.17 \cdot 0.4 + 0.24 \cdot \frac{0.016 \cdot 374}{\sqrt{11.3}} = 0.64 \text{ m}$$

$$\begin{aligned} \theta_y &= \varphi_y \cdot \frac{L_v}{3} + 0.0013 \cdot \left(1 + 1.5 \cdot \frac{H}{L_v}\right) + 0.13 \cdot \varphi_y \cdot \frac{d_b f_y}{\sqrt{f_c}} = \\ &= 0.0095 \cdot \frac{1.5}{3} + 0.0013 \cdot \left(1 + 1.5 \cdot \frac{0.4}{1.5}\right) + \\ &+ 0.13 \cdot 0.0095 \cdot \frac{0.016 \cdot 374}{\sqrt{11.3}} = 8.77 \cdot 10^{-3} = 0.50^\circ \end{aligned}$$

$$\begin{aligned} \theta_u &= \frac{1}{\gamma_{el}} \cdot \left[\theta_y + (\varphi_u - \varphi_y) \cdot \left(1 - \frac{L_{pl}}{2L_v}\right) \cdot L_{pl} \right] = \\ &= \frac{1}{1.5} \cdot \left[8.77 \cdot 10^{-3} + (0.027 - 0.0095) \cdot \left(1 - \frac{0.64}{2 \cdot 1.5}\right) \cdot 0.64 \right] = 0.012 = 0.67^\circ \end{aligned}$$

where bending and bending moment upon yielding of the tense steel bars are:

$$\varphi_y = 0.0095 \frac{1}{\text{m}} \qquad M_y = 96.72 \text{ kNm}$$

If we repeat the same calculations with 1 to 4 layers of reinforcement, we will obtain the results shown in table 2.3 and the moment-rotation diagrams shown in figure 2.15.



| | L_{pl} (m) | ϕ_y (m^{-1}) | θ_y ($^\circ$) | M_y (kNm) | θ_R ($^\circ$) | θ_u/θ_{u0} |
|----------|-----------------|--------------------------|----------------------------|----------------|----------------------------|------------------------|
| Unreinf. | 0.64 | 0.0095 | 0.50 | 96.72 | 0.67 | -- |
| 1 layer | 0.62 | 0.0093 | 0.49 | 97.14 | 1.09 | 1.61 |
| 2 layers | 0.60 | 0.0093 | 0.48 | 97.29 | 1.28 | 1.91 |
| 3 layers | 0.58 | 0.0092 | 0.47 | 97.40 | 1.43 | 2.10 |
| 4 layers | 0.57 | 0.0092 | 0.47 | 97.47 | 1.56 | 2.30 |

Table 4. Rotation capacity with respect to the chord. θ_{u0} : rotation capacity with respect to the chord without reinforcement.

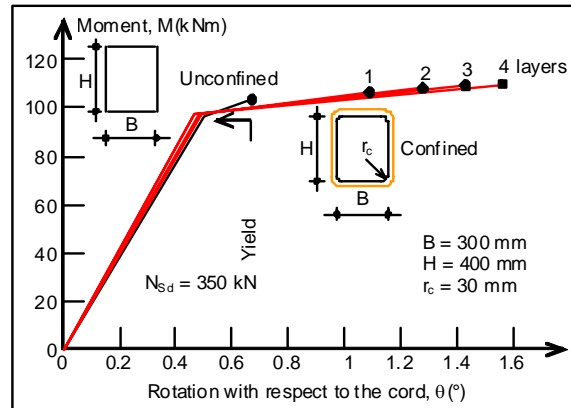


Figure 2.15. Diagrams illustrating moment-rotation with respect to the chord with different degrees of confinement



3. MASONRY STRUCTURES

3.1 Aims of reinforcement with FRM

Reinforcement of masonry structures in seismic zones with FRM composite materials is particularly effective for the following purposes:

- i) Increasing tensile strength in plane and out of plane of masonry panels (vertical wall elements and horizontal belts).
- ii) Increasing shear strength in plane of masonry panels (vertical wall elements and horizontal belts).
- iii) Inhibition of local collapse mechanisms.
- iv) Modification of the form of local collapse mechanisms, with a consequent increase in horizontal acceleration of their activation.

3.2 Vault reinforcement

Reinforcement of the intrados or extrados of a masonry vault subject to seismic forces with FRM composite materials may result, depending on the geometry of the reinforcement, in modification or prevention of the collapse mechanism of the unreinforced vault. In the first case, the reinforced structure will still collapse due to the mechanism, with acceleration of activation greater than that of the unreinforced structure; in the second case, the structure will collapse because it has reached the limit on the strength of the materials.

3.2.1 Reinforcement design

If reinforcement is installed in such a way that the reinforced structure will still collapse due to the mechanism, the extent of reinforcement may be designed to ensure that the spectral acceleration of activation of the new mechanism exceeds demand, expressed in terms of spectral acceleration, which may be calculated on the basis of the site, the soil properties and the geometry of the structure, according to the indications contained in point C8A.4 of [3]. The reinforcement section (number of layers) may later be designed by assessing the stress caused by normal force and the flexing moment associated with the acceleration of activation of the new collapse mechanism.

In the case of reinforcement installed in such a way as to impede all the collapse mechanisms, the reinforcement section (number of layers) may be designed on the basis of the stress caused by the normal force and bending moment associated with the seismic action taken into account in the project.

In both cases, on the basis of the indications contained in [1] the moment of resistance of a reinforced masonry section may be assessed by considering a constitutive relation for the masonry consisting of an initial linear elastic branch, up to a calculated compression strength of f_{md} , followed by a section subject to constant tension up to the point of deformation $\varepsilon_{mu} = 3.5\text{‰}$ and reinforcement of a linear elastic constitutive relation up to the substrate's delamination dilation (or, if smaller, the reinforcement's calculated tensile strength). Alternatively, we may simply use a "stress-block" approach.

3.2.1.1 Examples

Example 1. Reinforcement of the extrados of a barrel vault

Let us consider the vault-pier system shown in figure 3.1. $f_{mk} = 3 \text{ MPa}$ is the compression strength of the masonry. The calculation is performed with reference to unitary depth. The structure is subject not only to its own weight and the weight of the support, but to the load p_d distributed on the extrados of the support and situated in a seismic zone.

We initially calculate the acceleration of activation of the collapse mechanism in the unreinforced structure and then determine the size of reinforcement with FRM Ruredil XMesh C10/M25 to increase it.

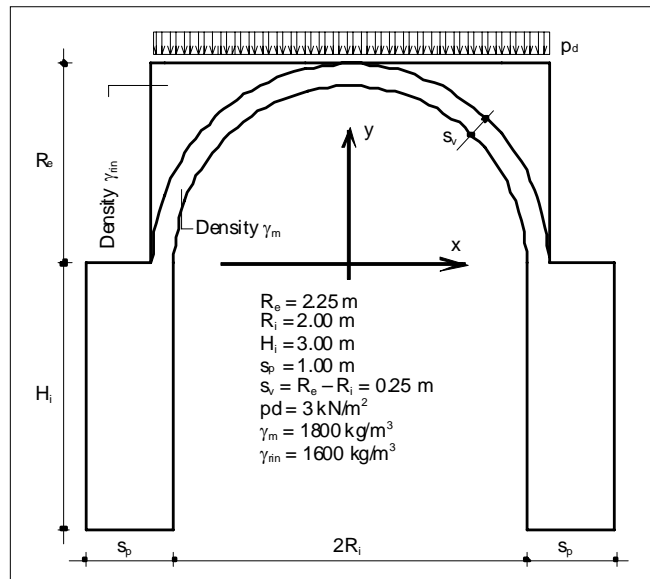


Figure 3.1. Vault-pier system.

Unreinforced structure

Horizontal collapse multiplier

Acting on the basis of the hypothesis that the masonry has infinite compression strength, with reference to figures 3.2 and 3.3, consider a collapse mechanism identified by the presence of 4 hinges. The structure thus remains subdivided into 3 free quoins to be rotated with respect to their centres of rotation. Vertical loads are considered to be applied to each of the 3 quoins (associated with their own weight, with support and with the uniformly distributed load) and a system of horizontal forces proportionate to the vertical loads through the unknown multiplier λ . The structure is in a condition of balance for as long as λ is small enough; it is not in balance if λ is sufficiently large. We are looking for the critical multiplier $\lambda = \lambda_c$ over which the structure no longer meets the condition of balance.

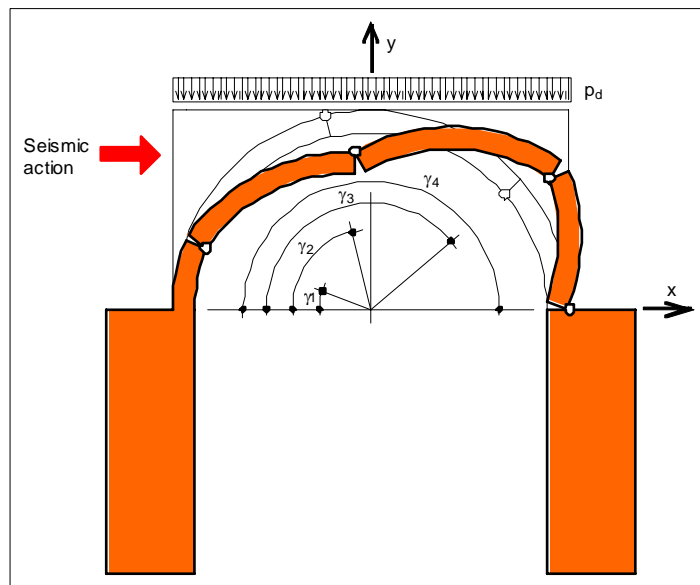


Figure 3.2. Collapse mechanism.

The system may achieve balance through the Principle of Virtual Work; the system is in equilibrium for as long as:

$$\sum_{i=1}^3 P_i \eta_i + \sum_{i=1}^3 P_{ri} \eta_{ri} + \sum_{i=1}^3 P_{di} \eta_{di} + \lambda \left(\sum_{i=1}^3 P_i \delta_i + \sum_{i=1}^3 P_{ri} \delta_{ri} + \sum_{i=1}^3 P_{di} \delta_{di} \right) \leq 0 \quad (3.1)$$

that is, as long as:



$$\lambda \leq - \frac{\sum_{i=1}^3 P_i \eta_i + \sum_{i=1}^3 P_{ri} \eta_{ri} + \sum_{i=1}^3 P_{di} \eta_{di}}{\sum_{i=1}^3 P_i \delta_i + \sum_{i=1}^3 P_{ri} \delta_{ri} + \sum_{i=1}^3 P_{di} \delta_{di}} \quad (3.2)$$

the critical multiplier for the mechanism taken into consideration is therefore:

$$\lambda_c = - \frac{\sum_{i=1}^3 P_i \eta_i + \sum_{i=1}^3 P_{ri} \eta_{ri} + \sum_{i=1}^3 P_{di} \eta_{di}}{\sum_{i=1}^3 P_i \delta_i + \sum_{i=1}^3 P_{ri} \delta_{ri} + \sum_{i=1}^3 P_{di} \delta_{di}} \quad (3.3)$$

where (figure 3.3):

- P_i is the weight of the i -th block ($i = 1, 2, 3$);
- P_{ri} is the weight of the support on the i -th block ($i = 1, 2, 3$);
- P_{di} is the result of the load uniformly distributed on the i -th block ($i = 1, 2, 3$);
- η_i is the vertical virtual shift in the application point of P_i ($i = 1, 2, 3$);
- η_{ri} is the vertical virtual shift in the application point of P_{ri} ($i = 1, 2, 3$);
- η_{di} is the vertical virtual shift in the application point of P_{di} ($i = 1, 2, 3$);
- δ_i is the horizontal virtual shift in the application point of P_i ($i = 1, 2, 3$);
- δ_{ri} is the horizontal virtual shift in the application point of P_{ri} ($i = 1, 2, 3$);
- δ_{di} is the horizontal virtual shift in the application point of P_{di} ($i = 1, 2, 3$).

In view of the mechanism shown in figures 3.2 and 3.3 for the hinges in the sections identified by:

$$\gamma_1 = 20.2^\circ \quad \gamma_2 = 76.6^\circ \quad \gamma_3 = 139.3^\circ \quad \gamma_4 = 180^\circ \quad (3.4)$$

the hinges are located at the coordinates:

$$\begin{aligned} x_1 &= -R_i \cos \gamma_1 = -1.88 \text{ m} & x_3 &= -R_i \cos \gamma_3 = 1.52 \text{ m} \\ y_1 &= R_i \sin \gamma_1 = 0.69 \text{ m} & y_3 &= R_i \sin \gamma_3 = 1.30 \text{ m} \\ x_2 &= -R_e \cos \gamma_2 = -0.52 \text{ m} & x_4 &= -R_e \cos \gamma_4 = 2.25 \text{ m} \\ y_2 &= R_e \sin \gamma_2 = 2.19 \text{ m} & y_4 &= R_e \sin \gamma_4 = 0 \text{ m} \end{aligned} \quad (3.5)$$

the weights of the three arch quoins and the coordinates of their application points are given by:

$$P_i = \gamma_m \frac{\gamma_{i+1} - \gamma_i}{2} \cdot (R_e^2 - R_i^2) \quad (3.6)$$

$$\begin{aligned} x_{gi} &= - \frac{4}{3 \cdot (\gamma_{i+1} - \gamma_i)} \cdot \frac{R_e^3 - R_i^3}{R_e^2 - R_i^2} \cdot \sin \frac{\gamma_{i+1} - \gamma_i}{2} \cdot \cos \frac{\gamma_{i+1} + \gamma_i}{2} \\ y_{gi} &= \frac{4}{3 \cdot (\gamma_{i+1} - \gamma_i)} \cdot \frac{R_e^3 - R_i^3}{R_e^2 - R_i^2} \cdot \sin \frac{\gamma_{i+1} - \gamma_i}{2} \cdot \sin \frac{\gamma_{i+1} + \gamma_i}{2} \end{aligned} \quad (3.7)$$

and are equal to:

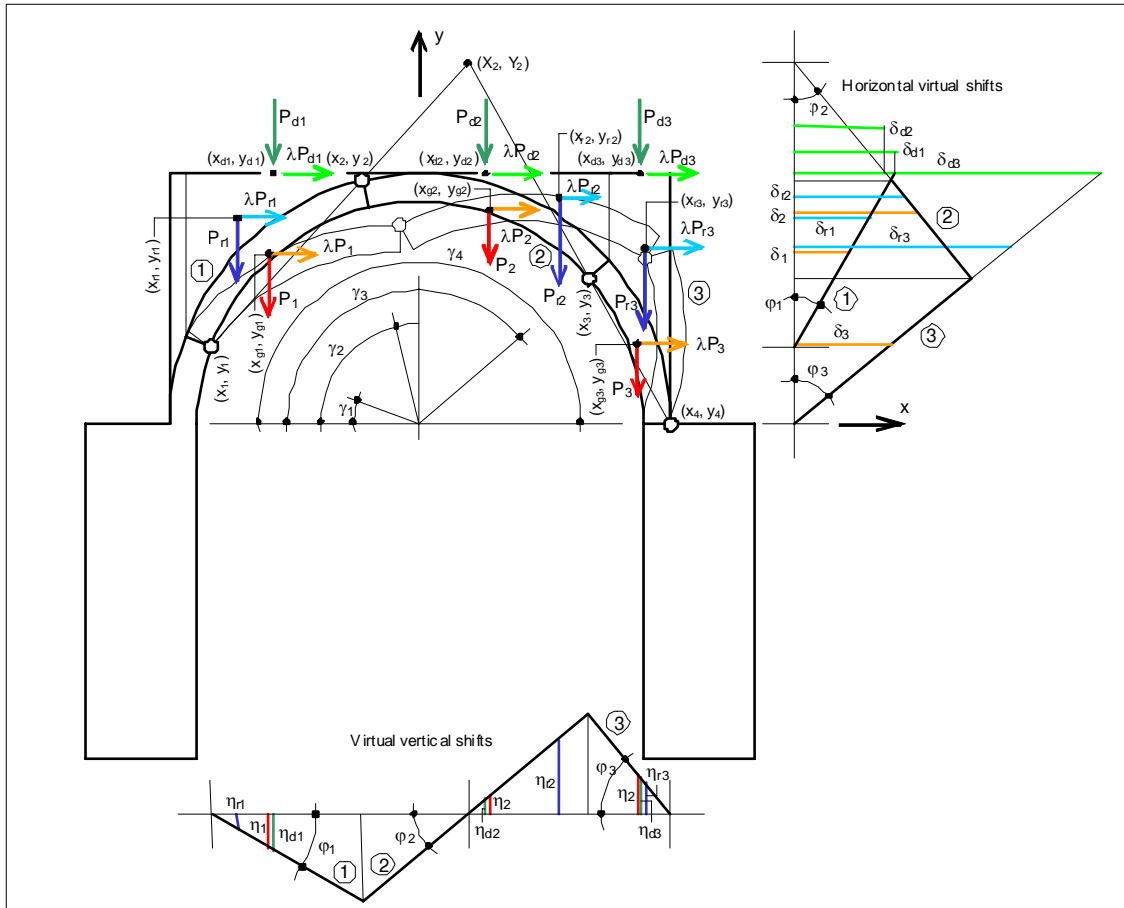


Figure 3.3. System of acting forces and virtual shifts.

$$\begin{array}{lll}
 P_1 = 9.22 \frac{\text{kN}}{\text{m}} & P_2 = 10.27 \frac{\text{kN}}{\text{m}} & P_3 = 6.66 \frac{\text{kN}}{\text{m}} \\
 x_{g1} = -1.36 \text{ m} & x_{g2} = 0.62 \text{ m} & x_{g3} = 1.95 \text{ m} \\
 y_{g1} = 1.53 \text{ m} & y_{g2} = 1.62 \text{ m} & y_{g3} = 0.72 \text{ m}
 \end{array} \quad (3.8)$$

the weight of the support on the three arch quins and the coordinates of their application points are given by

$$\begin{array}{ll}
 P_{ri} = \gamma_{rin} \cdot R_e^2 \cdot \int_{\gamma_i}^{\gamma_{i+1}} (\sin \gamma - \sin^2 \gamma) d\gamma & y_{ri} = \frac{\gamma_{rin} R_e^3}{2 \cdot P_{ri}} \cdot \int_{\gamma_i}^{\gamma_{i+1}} (\sin \gamma - \sin^3 \gamma) d\gamma \\
 x_{ri} = -\frac{\gamma_{rin} R_e^3}{P_{ri}} \cdot \int_{\gamma_i}^{\gamma_{i+1}} \sin \gamma \cos \gamma \cdot (1 + \sin \gamma) d\gamma
 \end{array} \quad (3.9)$$

and are equal to:

$$\begin{array}{lll}
 P_{r1} = 13.11 \frac{\text{kN}}{\text{m}} & P_{r2} = 6.58 \frac{\text{kN}}{\text{m}} & P_{r3} = 10.63 \frac{\text{kN}}{\text{m}} \\
 x_{r1} = -1.64 \text{ m} & x_{r2} = 1.25 \text{ m} & x_{r3} = 2.02 \text{ m} \\
 y_{r1} = 1.85 \text{ m} & y_{r2} = 2.03 \text{ m} & y_{r3} = 1.58 \text{ m}
 \end{array} \quad (3.10)$$

the results of the load distributed on the three arch quins and the coordinates of their application points may be calculated as follows:

$$\begin{array}{l}
 P_{di} = -p_d R_e \cdot (\cos \gamma_{i+1} - \cos \gamma_i) \\
 x_{di} = -\frac{R_e}{2} (\cos \gamma_{i+1} + \cos \gamma_i) \\
 y_{ri} = R_e
 \end{array} \quad (3.11)$$



and are equal to:

$$\begin{array}{lll} P_{d1} = 4.76 \frac{\text{kN}}{\text{m}} & P_{d2} = 6.69 \frac{\text{kN}}{\text{m}} & P_{d3} = 1.63 \frac{\text{kN}}{\text{m}} \\ x_{d1} = -1.32 \text{ m} & x_{d2} = 0.59 \text{ m} & x_{d3} = 1.98 \text{ m} \\ y_{d1} = 2.25 \text{ m} & y_{d2} = 2.25 \text{ m} & y_{d3} = 2.25 \text{ m} \end{array} \quad (3.12)$$

the centre of rotation of the second block has the following coordinates (figure 3.3):

$$\begin{aligned} X_2 &= \frac{(x_4 - x_3)[x_1(y_2 - y_1) + (y_3 - y_1)(x_2 - x_1)] - x_3(y_4 - y_3)(x_2 - x_1)}{(y_2 - y_1)(x_4 - x_3) - (y_4 - y_3)(x_2 - x_1)} = 0.43 \text{ m} \\ Y_2 &= y_1 + \frac{y_2 - y_1}{x_2 - x_1} \cdot (X_2 - x_1) = 3.24 \text{ m} \end{aligned} \quad (3.13)$$

If we arbitrarily determine the rotation φ_1 of the first block, the rotation of the second and third block will be (figure 3.3):

$$\varphi_2 = -\varphi_1 \cdot \frac{x_2 - x_1}{X_2 - x_2} = -1.42 \varphi_1 \quad \varphi_3 = \varphi_1 \cdot \frac{x_2 - x_1}{X_2 - x_2} \cdot \frac{x_3 - x_{2ass}}{x_4 - x_3} = 2.11 \varphi_1 \quad (3.14)$$

the shifts in the application points of forces are:

$$\begin{array}{ll} \eta_1 = \varphi_1 \cdot (x_{g1} - x_1) = 0.52 \cdot \varphi_1 & \delta_1 = \varphi_1 \cdot (y_{g1} - y_1) = 0.84 \cdot \varphi_1 \\ \eta_2 = \varphi_2 \cdot (x_{g2} - X_2) = -0.28 \cdot \varphi_1 & \delta_2 = \varphi_2 \cdot (y_{g2} - y_{2ass}) = 1.87 \cdot \varphi_1 \\ \eta_3 = \varphi_3 \cdot (x_{g3} - x_4) = -0.63 \cdot \varphi_1 & \delta_3 = \varphi_3 \cdot (y_{g3} - y_4) = 1.53 \cdot \varphi_1 \\ \eta_{r1} = \varphi_1 \cdot (x_{rin1} - x_1) = 0.24 \cdot \varphi_1 & \delta_{r1} = \varphi_1 \cdot (y_{rin1} - y_1) = 1.16 \cdot \varphi_1 \\ \eta_{r2} = \varphi_2 \cdot (x_{rin2} - x_{2ass}) = -1.18 \cdot \varphi_1 & \delta_{r2} = \varphi_2 \cdot (y_{rin2} - y_{2ass}) = 1.72 \cdot \varphi_1 \\ \eta_{r3} = \varphi_3 \cdot (x_{rin3} - x_4) = -0.49 \cdot \varphi_1 & \delta_{r3} = \varphi_3 \cdot (y_{rin3} - y_4) = 3.34 \cdot \varphi_1 \\ \eta_{d1} = \varphi_1 \cdot (x_{d1} - x_1) = 0.56 \cdot \varphi_1 & \delta_{d1} = \varphi_1 \cdot (y_{d1} - y_1) = 1.56 \cdot \varphi_1 \\ \eta_{d2} = \varphi_2 \cdot (x_{d2} - x_{2ass}) = -0.23 \cdot \varphi_1 & \delta_{d2} = \varphi_2 \cdot (y_{d2} - y_{2ass}) = 1.41 \cdot \varphi_1 \\ \eta_{d3} = \varphi_3 \cdot (x_{d3} - x_4) = -0.58 \cdot \varphi_1 & \delta_{d3} = \varphi_3 \cdot (y_{d3} - y_4) = 4.76 \cdot \varphi_1 \end{array} \quad (3.15)$$

If we apply (3.3) we therefore have the multiplier:

$$\lambda_c = 0.096 \quad (3.16)$$

This multiplier is dependent on the mechanism considered, and therefore the position of the hinges. In other words, if we change the position of the hinges (3.4) and repeat the procedure, we will get a different multiplier from the value (3.16). The structure's actual collapse multiplier is the smallest of all those corresponding to the kinetically admissible collapse mechanisms. It is therefore necessary to repeat the procedure described to obtain positions $\gamma_1, \gamma_2, \gamma_3, \gamma_4$ of the hinges determining the minimum collapse multiplier. This repetition has already been performed, so that the one represented by the hinges (3.4) is the effective collapse mechanism and the one expressed by (3.16) is the structure's effective collapse multiplier.

Location of pressure points

To confirm this, we may determine the location of pressure centres on the sections of the structure and check that it is always in the thickness or, in hinge sections, on the edge.

Constraining reactions in the extreme hinges (γ_1 e γ_4) can be determined using the system of equilibrium equations (figure 3.4):



$$\begin{cases}
 R_{vs} \cdot (x_2 - x_1) - H_s \cdot (y_2 - y_1) = P_1 \cdot (x_2 - x_{g1}) + P_{r1} \cdot (x_2 - x_{r1}) + \\
 \quad + P_{d1} \cdot (x_2 - y_{d1}) + \lambda_c \cdot [P_1 \cdot (y_2 - y_{g1}) + P_{r1} \cdot (y_2 - y_{r1}) + P_{d1} \cdot (y_2 - y_{d1})] \\
 R_{vd} \cdot (x_4 - x_2) - H_d \cdot (y_2 - y_4) = P_2 \cdot (x_{g2} - x_2) + P_3 \cdot (x_{g3} - x_2) + \\
 \quad + P_{r2} \cdot (x_{r2} - x_2) + P_{r3} \cdot (x_{r3} - x_2) + P_{d2} \cdot (x_{d2} - x_2) + \\
 \quad + P_{d3} \cdot (x_{d3} - x_2) + \lambda_c \cdot [P_2 \cdot (y_{g2} - y_2) + P_{r2} \cdot (y_{r2} - y_2) + \\
 \quad + P_{d2} \cdot (y_{d2} - y_2) + P_3 \cdot (y_{g3} - y_2) + P_{r3} \cdot (y_{r3} - y_2) + P_{d3} \cdot (y_{d3} - y_2)] \\
 R_{vs} + R_{vd} = \sum_{i=1}^3 (P_i + P_{ri} + P_{di}) \\
 H_s - H_d = -\lambda_c \cdot \sum_{i=1}^3 (P_i + P_{ri} + P_{di})
 \end{cases} \quad (3.17)$$

and are equal to:

$$R_{vs} = 29.72 \frac{\text{kN}}{\text{m}} \quad R_{vd} = 39.84 \frac{\text{kN}}{\text{m}} \quad H_s = 8.78 \frac{\text{kN}}{\text{m}} \quad H_d = 15.45 \frac{\text{kN}}{\text{m}} \quad (3.18)$$

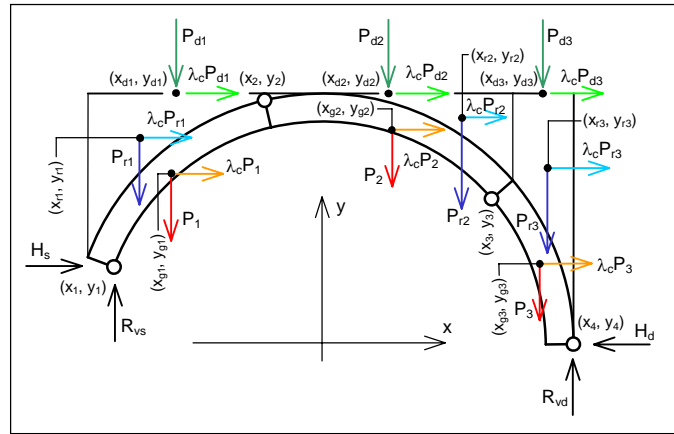


Figure 3.4. Reactions in the extreme hinges.

Bending moment in relation to the extrados of a generic section identified by γ is:

$$\begin{aligned}
 M(\gamma) = & R_{vs} \cdot (x_e(\gamma) - x_1) - H_s \cdot (y_e(\gamma) - y_1) + \\
 & - \left[(P(\gamma) - P(\gamma_1)) \cdot \left(x_e(\gamma) - \frac{x_g(\gamma) \cdot P(\gamma) - x_g(\gamma_1) \cdot P(\gamma_1)}{P(\gamma) - P(\gamma_1)} \right) \right] + \\
 & - \left[(P_r(\gamma) - P_r(\gamma_1)) \cdot \left(x_e(\gamma) - \frac{x_r(\gamma) \cdot P_r(\gamma) - x_r(\gamma_1) \cdot P_r(\gamma_1)}{P_r(\gamma) - P_r(\gamma_1)} \right) \right] + \\
 & - \left[(P_d(\gamma) - P_d(\gamma_1)) \cdot \left(x_e(\gamma) - \frac{x_d(\gamma) \cdot P_d(\gamma) - x_d(\gamma_1) \cdot P_d(\gamma_1)}{P_d(\gamma) - P_d(\gamma_1)} \right) \right] + \\
 & - \lambda_c \cdot \left[\left[(P(\gamma) - P(\gamma_1)) \cdot \left(y_e(\gamma) - \frac{y_g(\gamma) \cdot P(\gamma) - y_g(\gamma_1) \cdot P(\gamma_1)}{P(\gamma) - P(\gamma_1)} \right) \right] \right] + \\
 & + \left[(P_r(\gamma) - P_r(\gamma_1)) \cdot \left(y_e(\gamma) - \frac{y_r(\gamma) \cdot P_r(\gamma) - y_r(\gamma_1) \cdot P_r(\gamma_1)}{P_r(\gamma) - P_r(\gamma_1)} \right) \right] + \\
 & + [(P_d(\gamma) - P_d(\gamma_1)) \cdot (y_e(\gamma) - y_d)]
 \end{aligned} \quad (3.19)$$

where $y_d = y_{d1} = y_{d2} = y_{d3}$. Normal force, considered positive if it is compression force, in the generic section identified by γ is:

$$\begin{aligned}
 N(\gamma) = & [R_{vs} - (P(\gamma) + P_r(\gamma) + P_d(\gamma) - P(\gamma_1) - P_r(\gamma_1) - P_d(\gamma_1))] \cdot \cos \psi(\gamma) \\
 & + [H_s + \lambda_c \cdot (P(\gamma) + P_r(\gamma) + P_d(\gamma) - P(\gamma_1) - P_r(\gamma_1) - P_d(\gamma_1))] \cdot \sin \psi(\gamma)
 \end{aligned} \quad (3.20)$$

The functions of γ that appear in (3.19) and (3.20) are (figure 3.5):



- $x_e(\gamma)$: function associating the angle γ with the abscissa of the extrados of the section identified by γ ;
 $y_e(\gamma)$: function associating the angle γ with the ordinate of the extrados of the section identified by γ ;
 $P(\gamma)$: function associating the angle γ with the weight of the structure between the initial section and the section identified by γ ;
 $P_r(\gamma)$: function associating the angle γ with the weight of the support between the initial section and the section identified by γ ;
 $P_d(\gamma)$: function associating the angle γ with the result of the load distributed between the initial section and the section identified by γ ;
 $x_g(\gamma)$: function associating the angle γ with the abscissa of the point of application of $P(\gamma)$;
 $y_g(\gamma)$: function associating the angle γ with the ordinate of the point of application of $P(\gamma)$;
 $x_r(\gamma)$: function associating the angle γ with the abscissa of the point of application of $P_r(\gamma)$;
 $y_r(\gamma)$: function associating the angle γ with the ordinate of the point of application of $P_r(\gamma)$;
 $x_d(\gamma)$: function associating the angle γ with the abscissa of the point of application of $d(\gamma)$;
 $\psi(\gamma)$: function associating the angle γ with the inclination of the section identified by γ ;

and may be expressed as:

$$x_e(\gamma) = \begin{cases} -(R_i + s_p) & \text{if } \gamma_{ini} \leq \gamma < 0 \\ -R_e \cos \gamma & \text{if } 0 \leq \gamma \leq \pi \\ R_i + s_p & \text{if } \pi < \gamma \leq \pi - \gamma_i \end{cases} \quad y_e(\gamma) = \begin{cases} R_i \tan \gamma & \text{if } \gamma_{ini} \leq \gamma < 0 \\ R_e \sin \gamma & \text{if } 0 \leq \gamma \leq \pi \\ -R_i \tan \gamma & \text{if } \pi < \gamma \leq \pi - \gamma_i \end{cases} \quad (3.21)$$

$$P(\gamma) = \gamma_m \cdot \begin{cases} (y_e(\gamma) + H_i) \cdot s_p & \text{if } \gamma_{ini} \leq \gamma < 0 \\ H_i s_p + \frac{\gamma}{2} \cdot (R_e^2 - R_i^2) & \text{if } 0 \leq \gamma \leq \pi \\ H_i s_p + P_v - y_e(\gamma) \cdot s_p & \text{if } \pi < \gamma \leq \pi - \gamma_{ini} \end{cases} \quad (3.22)$$

$$P_r(\gamma) = \gamma_{rin} \cdot R_e \cdot \int_{\gamma_{ini}}^{\gamma} h_r(\gamma) \cdot \sin \gamma d\gamma \quad P_d(\gamma) = p_d \cdot \begin{cases} 0 & \text{if } \gamma_{ini} \leq \gamma < 0 \\ x_e(\gamma) + R_e & \text{if } 0 \leq \gamma \leq \pi \\ 2R_e & \text{if } \pi < \gamma \leq \pi - \gamma_i \end{cases}$$

$$x_g(\gamma) = \begin{cases} x_{gp} & \text{if } \gamma_{ini} \leq \gamma < 0 \\ \frac{1}{P(\gamma)} \cdot \left[P_p x_{gp} - \frac{4}{3\gamma} \cdot (P(\gamma) - P_p) \cdot \frac{R_e^3 - R_i^3}{R_e^2 - R_i^2} \cdot \sin \frac{\gamma}{2} \cos \frac{\gamma}{2} \right] & \text{if } 0 \leq \gamma \leq \pi \\ \frac{1}{P(\gamma)} \cdot \left[P_p x_{gp} + \gamma_m \cdot y_e(\gamma) \cdot s_p x_{gp} \right] & \text{if } \pi < \gamma \leq \pi \end{cases} \quad (3.23)$$

$$y_g(\gamma) = \begin{cases} \frac{y_e(\gamma) - H_i}{2} & \text{if } \gamma_{ini} \leq \gamma < 0 \\ \frac{1}{P(\gamma)} \cdot \left[P_p y_{gp} + \frac{4}{3\gamma} \cdot (P(\gamma) - P_p) \cdot \frac{R_e^3 - R_i^3}{R_e^2 - R_i^2} \cdot \sin^2 \frac{\gamma}{2} \right] & \text{if } 0 \leq \gamma \leq \pi \\ \frac{1}{P(\gamma)} \cdot \left[P_p y_{gp} + P_v y_{gv} - \gamma_m y_e^2(\gamma) \frac{s_p}{2} \right] & \text{if } \pi < \gamma \leq \pi \end{cases}$$



$$x_r(\gamma) = \begin{cases} -R_e & \text{if } \gamma_{ini} \leq \gamma < 0 \\ \frac{\gamma_{rin} \cdot R_e}{P_r(\gamma)} \cdot \int_0^\gamma h_r(\gamma) \cdot x_e(\gamma) \cdot \sin \gamma & \text{if } 0 \leq \gamma \leq \pi \\ 0 & \text{if } \pi < \gamma \leq \pi - \gamma_{ini} \end{cases}$$

$$y_r(\gamma) = \begin{cases} \frac{R_e}{2} & \text{if } \gamma_{ini} \leq \gamma < 0 \\ \frac{\gamma_{rin} \cdot R_e}{P_r(\gamma)} \cdot \int_0^\gamma h_r(\gamma) \cdot \left(y_e(\gamma) + \frac{h_r(\gamma)}{2} \right) \cdot \sin \gamma & \text{if } 0 \leq \gamma \leq \pi \\ y_{gr} & \text{if } \pi < \gamma \leq \pi \end{cases} \quad (3.24)$$

$$x_d(\gamma) = \begin{cases} -R_e & \text{if } \gamma_{ini} \leq \gamma < 0 \\ -R_e \frac{\cos \gamma + 1}{2} & \text{if } 0 \leq \gamma \leq \pi \\ 0 & \text{if } \pi < \gamma \leq \pi - \gamma_{ini} \end{cases} \quad \psi(\gamma) = \begin{cases} 0 & \text{if } \gamma_{ini} \leq \gamma < 0 \\ \gamma & \text{if } 0 \leq \gamma \leq \pi \\ \pi & \text{if } \pi < \gamma \leq \pi - \gamma_{ini} \end{cases} \quad (3.25)$$

where $h_r(\gamma)$ is the height of the support on the section identified by γ (figure 3.5):

$$h_r(\gamma) = \begin{cases} 0 & \text{if } \gamma_{ini} \leq \gamma < 0 \\ R_e - y_e(\gamma) & \text{if } 0 \leq \gamma \leq \pi \\ 0 & \text{if } \pi < \gamma \leq \pi - \gamma_{ini} \end{cases} \quad (3.26)$$

γ_{ini} is the value of γ corresponding to the base section of the left pier:

$$\gamma_{ini} = -a \tan\left(\frac{H_i}{R_i}\right) = -56.31^\circ \quad (3.27)$$

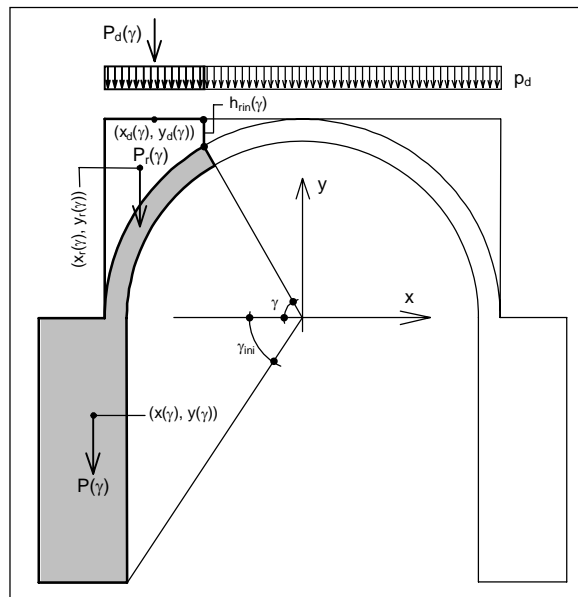


Figure 3.5. Functions of γ .

P_p and x_{gp} represent the weight of each pier and the abscissa of the centre of gravity of the left pier, respectively:



$$P_p = \gamma_m s_p H_i = 52.96 \frac{\text{kN}}{\text{m}} \quad x_{gp} = -\left(R_i + \frac{s_p}{2}\right) = -2.5 \text{ m} \quad (3.28)$$

P_v and y_{gv} represent the weight of the vault and the ordinate of its centre of gravity:

$$P_v = \gamma_m \frac{\pi}{2} (R_e^2 - R_i^2) = 29.46 \frac{\text{kN}}{\text{m}} \quad y_{gv} = \frac{4}{3\pi} \cdot \frac{R_e^3 - R_i^3}{R_e^2 - R_i^2} = 1.35 \text{ m} \quad (3.29)$$

P_{tr} and y_{gr} represent the total weight of the support and the ordinate of the centre of gravity of its volume:

$$P_{tr} = \frac{\gamma_{rin} R_e^2 \cdot (4 - \pi)}{2} = 34.09 \frac{\text{kN}}{\text{m}} \quad y_{gr} = \frac{\gamma_{rin} R_e^3}{3P_{tr}} = 1.75 \text{ m} \quad (3.30)$$

The distance from the centre of pressure of the extrados in the section γ is:

$$u(\gamma) = \frac{M(\gamma)}{N(\gamma)} \quad (3.31)$$

while the location of pressure centres on the structure's plane is given by the parametric equations:

$$x_p(\gamma) = x_e(\gamma) - u(\gamma) \cos(\psi(\gamma)) \quad y_e(\gamma) + u(\gamma) \cdot \sin(\psi(\gamma)) \quad (3.32)$$

The location of the pressure centres expressed by (3.32) is traced in figure 3.6.

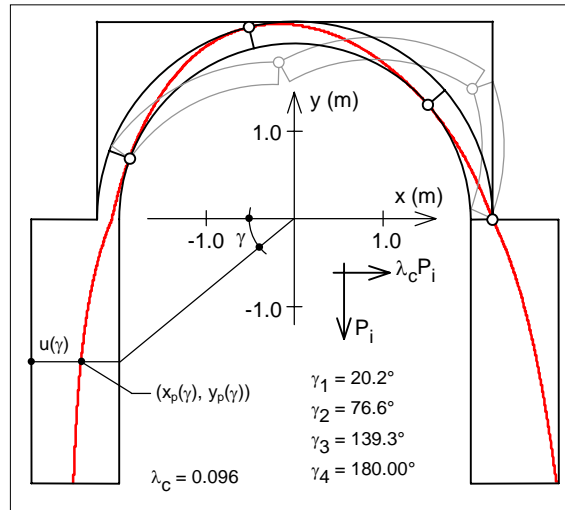


Figure 3.6. Location of pressure centres.

Acceleration of activation of the mechanism

On the basis of the set-up in point C8A.4 of [3], the mass participating in the collapse mechanism shown in figure 3.3 is the product of:

$$M^* = \frac{\left(\sum_{i=1}^3 P_i \cdot \delta_i + \sum_{i=1}^3 P_{ri} \cdot \delta_{ri} + \sum_{i=1}^3 P_{di} \cdot \delta_{di} \right)^2}{g \left(\sum_{i=1}^3 P_i \cdot \delta_i^2 + \sum_{i=1}^3 P_{ri} \cdot \delta_{ri}^2 + \sum_{i=1}^3 P_{di} \cdot \delta_{di}^2 \right)} = \frac{55.59 \text{ kN}}{g \text{ m}} \quad (3.33)$$

where the weights P_i , P_{ri} and P_{di} ($i = 1, 2, 3$) and the corresponding horizontal shifts are given by (3.8) – (3.15).

The fraction of mass participating is therefore:

$$e^* = \frac{gM^*}{P_{tot}} = 0.8 \quad (3.34)$$

where P_{tot} is the total weight of the masses involved in the mechanism:



$$P_{\text{tot}} = \sum_{i=1}^3 P_i + \sum_{i=1}^3 P_{ri} + \sum_{i=1}^3 P_{di} = 69.56 \frac{\text{kN}}{\text{m}} \quad (3.35)$$

Lastly, spectral acceleration of activation of the mechanism shown in figure 3.3 is:

$$a_0^* = \frac{\lambda_c g}{e^* \cdot FC} = 0.09 \text{ g} \quad (3.36)$$

where the confidence factor FC is assumed to be 1.35.

Reinforced structure

We intend to reinforce the structure so as to change its collapse mechanism and increase the corresponding horizontal multiplier. Note that the collapse mechanism in the unreinforced structure (figure 3.3) does not involve the piers, which are capable of supplying the vault with the necessary horizontal reaction (thrust) without overturning.

Let us consider the reinforcement device shown in figure 3.7, in which Ruredil XMesh/M25 composite material is applied all over the extrados of the vault. This ensures that there cannot be intrados hinges in the sections of the vault, but only in those of the piers, which will therefore be involved in the new collapse mechanism. The collapse multiplier of the reinforced structure may therefore still be determined using (3.3) in which the quantities (weights and shifts) are consistent with a new collapse mechanism in which the intrados hinges may only be located in the section of the piers, while the extrados hinges, which are not impeded by the reinforcement, may be placed in any position.

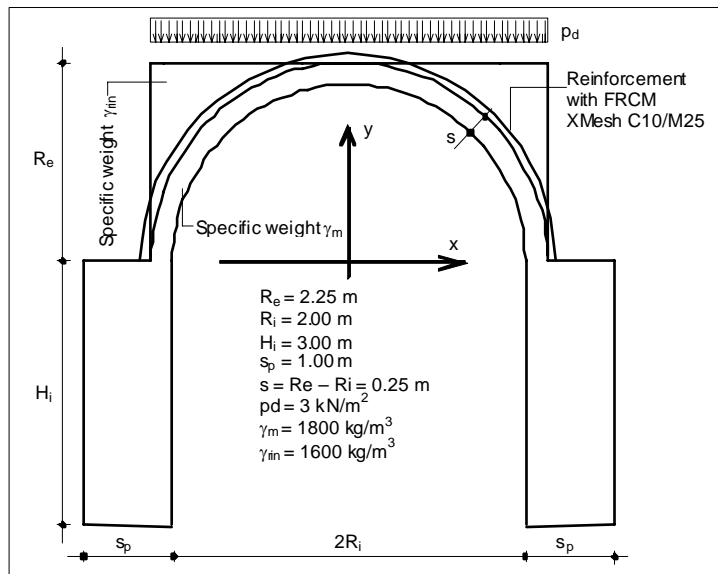


Figure 3.7. Location of FRCM reinforcement.

Horizontal collapse mechanism

Let us then consider the collapse mechanism shown in figures 3.8 and 3.9, with the hinges in the sections:

$$\gamma_1 = 0^\circ \quad \gamma_2 = 56.67^\circ \quad \gamma_3 = 180^\circ \quad \gamma_4 = \pi - \gamma_{ini} = 236.31^\circ \quad (3.37)$$

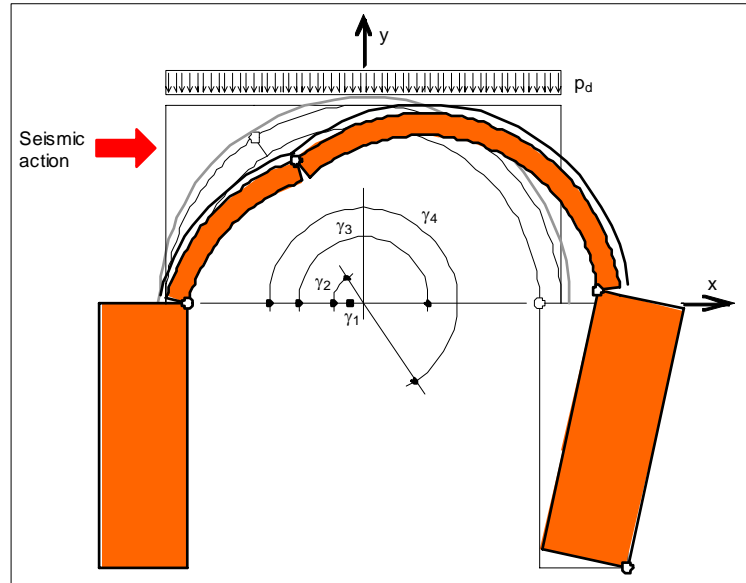


Figure 3.8. Collapse mechanism of the structure with FRCM reinforcement.

In relation to this mechanism, the hinges are located at the coordinates (figure 3.9):

$$\begin{aligned}
 x_1 &= -R_i = -2.00 \text{ m} & x_3 &= R_i = 2.00 \text{ m} \\
 y_1 &= 0 & y_3 &= 0 \\
 x_2 &= -R_e \cos \gamma_2 = -1.24 \text{ m} & x_4 &= R_i + s_p = 3.00 \text{ m} \\
 y_2 &= R_e \sin \gamma_2 = 1.88 \text{ m} & y_4 &= -H_i = -3.00 \text{ m}
 \end{aligned} \tag{3.38}$$

the weights and centres of gravity of the first two quoin are also determined according to (3.6), while the weight and centre of gravity of the third block are relative to the right pier only:

$$\begin{aligned}
 P_1 &= 9.28 \frac{\text{kN}}{\text{m}} & P_2 &= 20.18 \frac{\text{kN}}{\text{m}} & P_3 &= \gamma_m H_i s_p = 52.96 \frac{\text{kN}}{\text{m}} \\
 x_{g1} &= -1.80 \text{ m} & x_{g2} &= 0.83 \text{ m} & x_{g3} &= R_i + \frac{s_p}{2} = 2.50 \text{ m} \\
 y_{g1} &= 0.97 \text{ m} & y_{g2} &= 1.53 \text{ m} & y_{g3} &= -\frac{H_i}{2} = -1.50 \text{ m}
 \end{aligned} \tag{3.39}$$

the weights of the support on the first two quoin are also determined by (3.9), while the weight of the support on the third block is null:

$$\begin{aligned}
 P_{r1} &= 14.74 \frac{\text{kN}}{\text{m}} & P_{r2} &= 19.35 \frac{\text{kN}}{\text{m}} & P_{r3} &= 0 \\
 x_{r1} &= -1.86 \text{ m} & x_{r2} &= 1.43 \text{ m} \\
 y_{r1} &= 1.69 \text{ m} & y_{r2} &= 1.79 \text{ m}
 \end{aligned} \tag{3.40}$$

the results of the load distributed on the first two quoin and the coordinates of their points of application are also determined by (3.11), while the load distributed on the third block is null:

$$\begin{aligned}
 P_{d1} &= 3.04 \frac{\text{kN}}{\text{m}} & P_{d2} &= 10.46 \frac{\text{kN}}{\text{m}} & P_{d3} &= 0 \\
 x_{d1} &= -1.74 \text{ m} & x_{d2} &= 0.51 \text{ m} \\
 y_{d1} &= 2.25 \text{ m} & y_{d2} &= 2.25 \text{ m}
 \end{aligned} \tag{3.41}$$

the centre of rotation of the second is also determined according to (3.13):

$$\begin{aligned}
 X_2 &= 0.20 \text{ m} & Y_2 &= 5.41 \text{ m}
 \end{aligned} \tag{3.42}$$

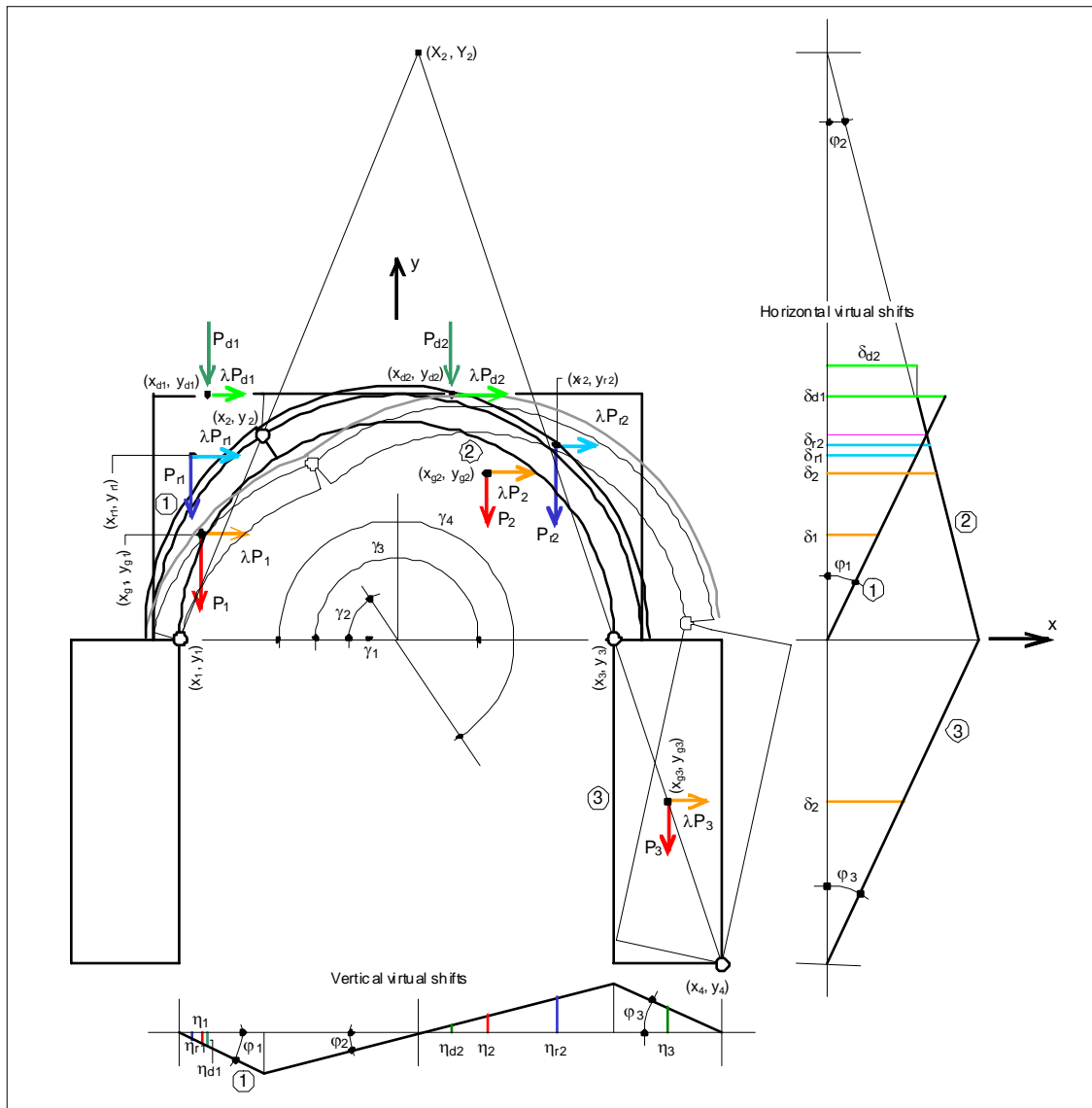


Figure 3.9. System of acting forces and virtual shifts of the FRCM reinforced structure.

Having arbitrarily determined the rotation φ_1 of the first block, the rotations of the second and third block can also be determined with (3.14):

$$\varphi_2 = -0.53 \varphi_1 \quad \varphi_3 = 0.96 \varphi_1 \quad (3.43)$$

the shifts in the points of application of forces, once again determined according to (3.15), are therefore:

$$\begin{aligned} \eta_1 &= 0.20 \cdot \varphi_1 & \eta_2 &= -0.34 \cdot \varphi_1 & \eta_3 &= -0.48 \cdot \varphi_1 \\ \eta_{r1} &= 0.13 \cdot \varphi_1 & \eta_{r2} &= -0.66 \cdot \varphi_1 & & \\ \eta_{d1} &= 0.26 \cdot \varphi_1 & \eta_{d2} &= -0.17 \cdot \varphi_1 & & \\ \delta_1 &= 0.97 \cdot \varphi_1 & \delta_2 &= 2.07 \cdot \varphi_1 & \delta_3 &= 1.44 \cdot \varphi_1 \\ \delta_{r1} &= 1.69 \cdot \varphi_1 & \delta_{r2} &= 1.93 \cdot \varphi_1 & & \\ \delta_{d1} &= 2.25 \cdot \varphi_1 & \delta_{d2} &= 1.68 \cdot \varphi_1 & & \end{aligned} \quad (3.44)$$

If we apply (3.3) we therefore obtain the multiplier:

$$\lambda_c = 0.197 \quad (3.45)$$

which is about double the one for the unreinforced structure (the mechanism in figure 3.2).

Here too, the multiplier depends on the mechanism taken into consideration, and therefore the position of the hinges. If we change the position of the hinges (3.37), always complying with the restrictions imposed by the reinforcement, and repeating the procedure described, we will find a different multiplier from the value of (3.45). The effective collapse multiplier of the reinforced structure may be found by minimising the collapse



multiplier with respect to the positions of the hinges $\gamma_1, \gamma_2, \gamma_3, \gamma_4$, always in compliance with the restrictions created by the reinforcement. This operation was performed before, and so the one represented by the hinges (3.37) is the effective collapse mechanism of the reinforced structure and the one expressed by (3.45) is the effective collapse multiplier.

Location of pressure centres

To confirm this, we may determine the location of centres of pressure on the sections of the structure and check that it:

- i) always lies in the thickness in unreinforced sections or on the edge of hinge sections;
- ii) lies in the thickness or intrados of sections with a reinforced extrados; in the latter case, tensile in the reinforcement can guarantee equilibrium.

The constraining reactions (figure 3.10) in the end hinges (γ_1 e γ_4) can also be determined using the system (3.17) and entering the quantities for the collapse mechanism in it (3.37), equal to:

$$R_{vs} = 32.13 \frac{\text{kN}}{\text{m}} \quad R_{vd} = 97.88 \frac{\text{kN}}{\text{m}} \quad H_s = 3.39 \frac{\text{kN}}{\text{m}} \quad H_d = 29.02 \frac{\text{kN}}{\text{m}} \quad (3.46)$$

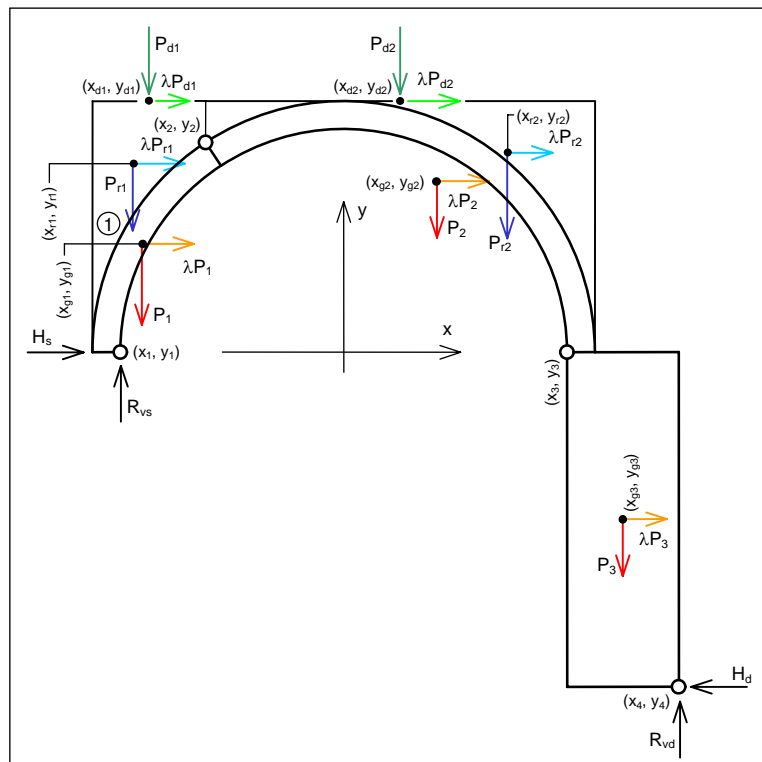


Figure 3.10. Reactions in the end hinges of a structure reinforced with FRM.

Bending moment in relation to the extrados and normal force in the generic section identified by γ are also expressed by (3.19) and (3.20), with the parameters corresponding to the new collapse mechanism. The resulting location of the pressure centres, once again expressed by (3.31) and (3.32), is shown in figure 3.11.

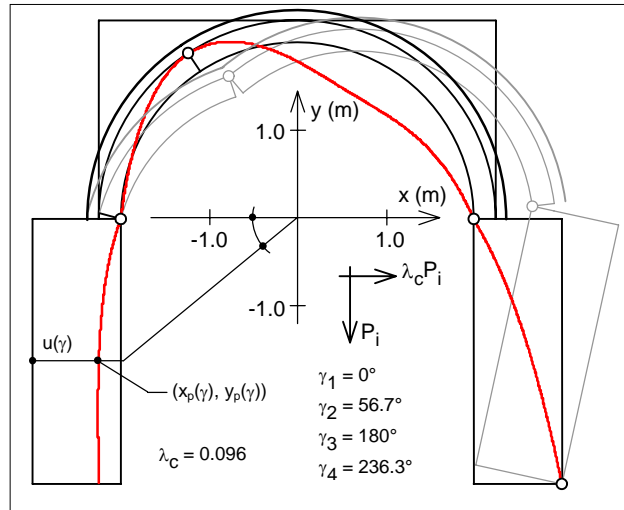


Figure 3.11.

Acceleration of the activation of the mechanism

Following the set-up of point C8A.4 in [3] for the reinforced section too, the mass participating in the collapse mechanism in figure 3.9 is calculated as follows:

$$M^* = \frac{\left(\sum_{i=1}^3 P_i \cdot \delta_i + \sum_{i=1}^2 P_{ri} \cdot \delta_{ri} + \sum_{i=1}^2 P_{di} \cdot \delta_{di} \right)^2}{g \left(\sum_{i=1}^3 P_i \cdot \delta_i^2 + \sum_{i=1}^2 P_{ri} \cdot \delta_{ri}^2 + \sum_{i=1}^2 P_{di} \cdot \delta_{di}^2 \right)} = \frac{125.40}{g} \frac{\text{kN}}{\text{m}} \quad (3.47)$$

where weights P_i , P_{ri} e P_{di} ($i = 1, 2, 3$) and the corresponding horizontal shifts are the product of (3.39) - (3.44).

The fraction of the mass participating is therefore:

$$e^* = \frac{gM^*}{P_{\text{tot}}} = 0.97 \quad (3.48)$$

where P_{tot} is the total weight of the masses involved in the mechanism shown in figure 3.9:

$$P_{\text{tot}} = \sum_{i=1}^3 P_i + \sum_{i=1}^2 P_{ri} + \sum_{i=1}^2 P_{di} = 130.01 \frac{\text{kN}}{\text{m}} \quad (3.49)$$

Spectral acceleration of activation of the mechanism in the figure is therefore:

$$a_0^* = \frac{\lambda_c g}{e^* \cdot FC} = 0.151 g \quad (3.50)$$

where the confidence factor FC is once more assumed to be 1.35. This acceleration of activation is 67% greater than that of the unreinforced structure. Note that, in order to increase the horizontal collapse multiplier even more, and therefore spectral acceleration of activation of the mechanism, it would be necessary to intervene by reinforcing the intrados of the vault or the piers as well.

At this point we may express an opinion as to the suitability of acceleration of activation of the mechanism by comparing this acceleration with demand, which basically depends on the site on which the construction stands, as described in point C8A.4 of [3].

Stress (moment and normal force)

The bending moment and normal force described in (3.19) and (3.20) appear in figures 3.12 and 3.13. Figure 3.12 also shows bending moment $M_{Sd}(\gamma)$, calculated with respect to the centre of gravity of the sections produced by:



$$M_{Sd}(\gamma) = M(\gamma) + N(\gamma) \frac{s(\gamma)}{2} \quad \text{with} \quad s(\gamma) = \begin{cases} s_p & \text{if } \gamma_{ini} \leq \gamma < 0 \\ s_v & \text{if } 0 \leq \gamma \leq \pi \\ s_p & \text{if } \pi < \gamma \leq \pi - \gamma_{ini} \end{cases} \quad (3.51)$$

In each of the reinforced sections, the section of the reinforcement must be determined in relation to this stress. For example, consider the following when checking:

- i) the section in which the eccentricity of normal force is greatest (in the modulus);
- ii) the section in which moment $M_{Sd}(\gamma)$ is greatest (in the modulus).

If we study the location of the pressure centres (3.31) we may decide that the section in which normal force acts with maximum eccentricity will be identified by (figure 3.12):

$$\gamma_{v1} = 121^\circ \quad (3.52)$$

the corresponding stress is:

$$M_{Sd1} = |M_{SD}(\gamma_{v1})| = 11.56 \frac{\text{kNm}}{\text{m}} \quad N_{Sd1} = N(\gamma_{v1}) = 19.81 \frac{\text{kN}}{\text{m}} \quad (3.53)$$

If we examine the moment diagram (3.51) we may determine that the section with maximum bending moment is identified by (figure 3.12):

$$\gamma_{v2} = 154^\circ \quad (3.54)$$

the corresponding stresses are:

$$M_{Sd2} = |M_{SD}(\gamma_{v2})| = 15.69 \frac{\text{kNm}}{\text{m}} \quad N_{Sd2} = N(\gamma_{v2}) = 38.32 \frac{\text{kN}}{\text{m}} \quad (3.55)$$

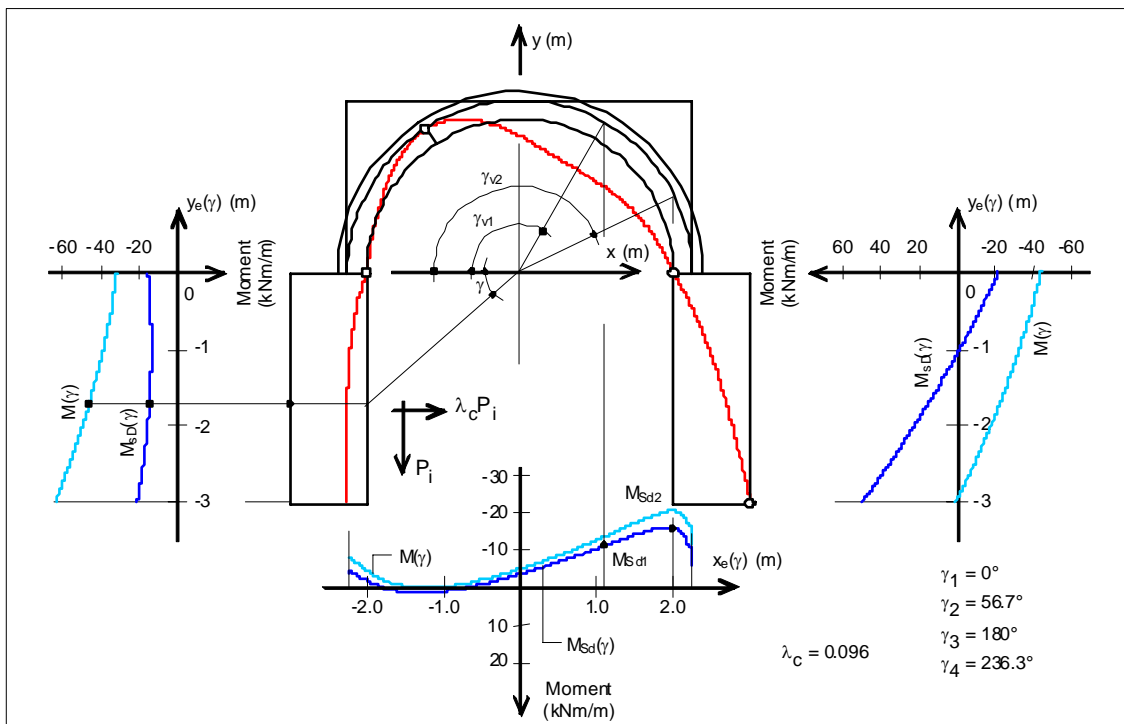


Figure 3.12. Bending moment.

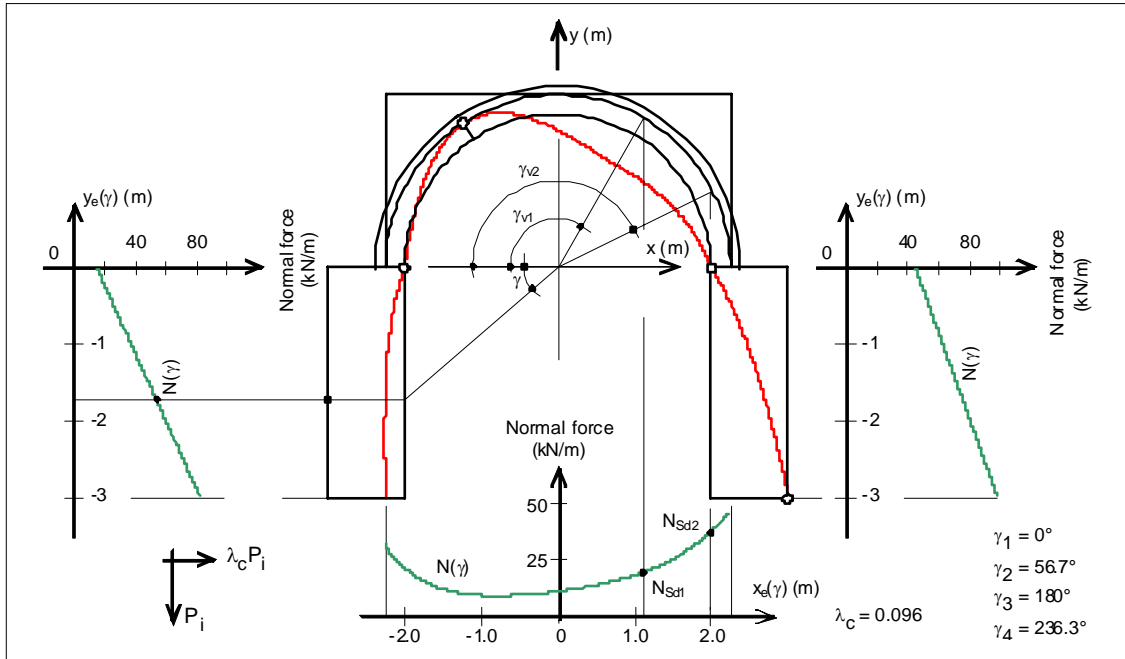


Figure 3.13. Normal force.

Reinforcement section

Supposing we reinforce the vault extrados as shown in figure 3.7, with two layers of FRMC Ruredil XMesh C10/M25. The reinforcement section is therefore:

$$A_f = 2 \cdot t_{1f} = 2 \cdot 0.047 \cdot 1000 = 94 \frac{\text{mm}^2}{\text{m}} \quad (3.56)$$

where $t_{1f} = 0.047$ mm is the nominal thickness of the individual layer of reinforcement.

Taking into account the phenomenon of delamination, we consider a calculated dilation of the reinforcement of $\varepsilon_{fd} = 3\%$. We then determine the section of the vault reinforced against stresses (3.53) and (3.55).

If we adopt the “stress-block” approach, and supposing the section to have broken when the reinforcement’s ultimate dilation point was reached (figure 3.14), for section γ_{v1} we will have:

$$M_{Rd1} = \frac{\alpha\beta \cdot f_{md}x}{2} \cdot (s - \beta x) + E_f \varepsilon_{fd} \frac{s}{2} = 16.39 \frac{\text{kNm}}{\text{m}} \quad (3.57)$$

where x is the distance of the neutral axis from the compressed edge:

$$x = \frac{A_f E_f \varepsilon_{fd} + N_{Sd1}}{\alpha\beta f_{md}} = 85.8 \text{ mm} \quad (3.58)$$

and as α and β are defined in figure 3.14, $E_f = 240000$ MPa the modulus of elasticity of the reinforcement fibers is:

$$f_{md} = \frac{f_{mk}}{\gamma_M} = 1.5 \text{ MPa} \quad (3.59)$$

the calculated compression strength of the masonry, assessed taking into account a partial safety coefficient of $\gamma_M = 2$.

with a maximum masonry deformation of:

$$\varepsilon_m = \varepsilon_{fd} \cdot \frac{x}{s - x} = 1.57 \text{ ‰} \quad (3.60)$$

less than $\varepsilon_{mu} = 3.5\%$, we may confirm the assumption of breakage on the reinforced side.

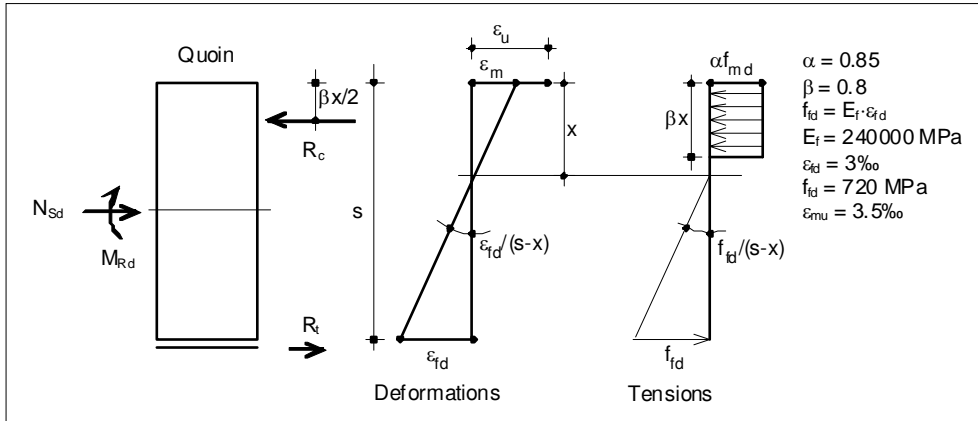


Figure 3.14. Tension status of the section.

In relation to section γ_{v2} , we will have:

$$M_{Rd2} = \frac{\alpha\beta \cdot f_{md}x}{2} \cdot (s - \beta x) + E_f \varepsilon_{fd} \frac{s}{2} = 17.30 \frac{\text{kNm}}{\text{m}} \quad (3.61)$$

where the distance x of the neutral axis from the compressed edge is:

$$x = \frac{A_f E_f \varepsilon_{fd} + N_{Sd2}}{\alpha \beta f_{md}} = 103.9 \text{ mm} \quad (3.62)$$

In this case, the maximum deformation of the masonry is:

$$\varepsilon_m = \varepsilon_{fd} \cdot \frac{x}{s - x} = 2.13 \text{ ‰} \quad (3.63)$$

which is once again less than $\varepsilon_{mu} = 3.5\text{‰}$.

Figure 3.15 illustrates verification of all the reinforced sections of the vault. It shows on the plane (N, M) the dominion of resistance of the reinforced section and the location of points $(N_{Sd}(\gamma), M_{Sd}(\gamma))$, with γ between 0 and π .

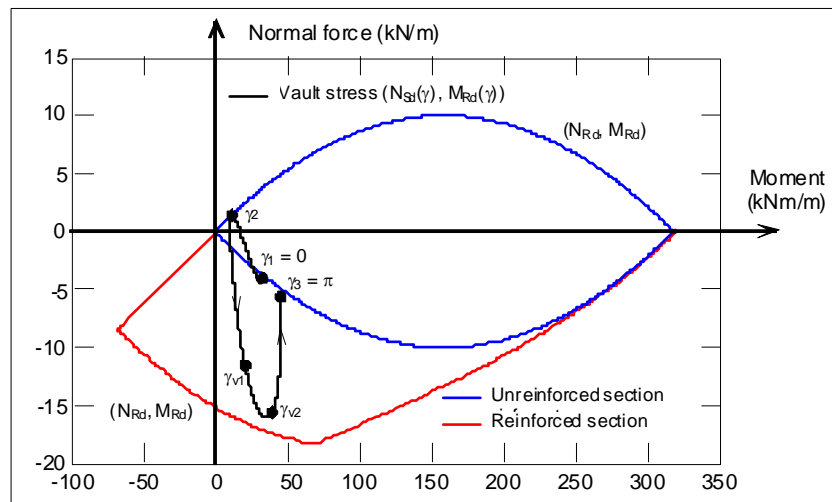


Figure 3.15. Domain of resistance and location of stresses on the vault.

Shear

In relation to the reinforced structure, under the mechanism condition shear of the generic section identified by γ will be:

$$V(\gamma) = [R_{vs} - (P(\gamma) + P_r(\gamma) + P_d(\gamma) - P(\gamma_1) - P_r(\gamma_1) - P_d(\gamma_1))] \cdot \sin \psi(\gamma) - [H_s + \lambda_c \cdot (P(\gamma) + P_r(\gamma) + P_d(\gamma) - P(\gamma_1) - P_r(\gamma_1) - P_d(\gamma_1))] \cdot \cos \psi(\gamma) \quad (3.64)$$



Considering the contribution of both friction and cohesion to shear strength, the shear strength of the generic section identified may be estimated as:

$$V_{Rd}(\gamma) = \frac{1}{\gamma_{Rd}} \left[0.9 \cdot s(\gamma) \cdot f_{vd0} + \frac{\mu_k}{\gamma_M} \cdot R_c(\gamma) \right] \quad (3.65)$$

where:

- γ_{Rd} is the partial model coefficient, assumed to be 1.2;
- $s(\gamma)$ is the thickness of the structure in section γ (the second of (3.51));
- f_{vd0} is the calculated shear strength of the masonry in the absence of normal force;
- μ_k is the characteristic value of the masonry friction coefficient;
- γ_M is the partial safety coefficient of the masonry ($\gamma_M = 2$);
- $R_c(\gamma)$ is the result of compression of the masonry, which may be estimated as approximately:

$$R_c(\gamma) = \begin{cases} N(\gamma) & \text{if } -s(\gamma) \leq u(\gamma) \leq \text{centre of pressure in the section} \\ N(\gamma) \frac{u(\gamma)}{s(\gamma)} & \text{if } u(\gamma) < -s(\gamma) \text{ (centre of pressure outside the section)} \end{cases} \quad (3.66)$$

Shear strength (3.65) must be greater than the shear stress acting in each section (3.64). Comparison of shear stress and shear strength (3.65) obtained by assuming $f_{vd0} = 0.06$ MPa and $\mu_k = 0.4$ is shown in figure 3.16.

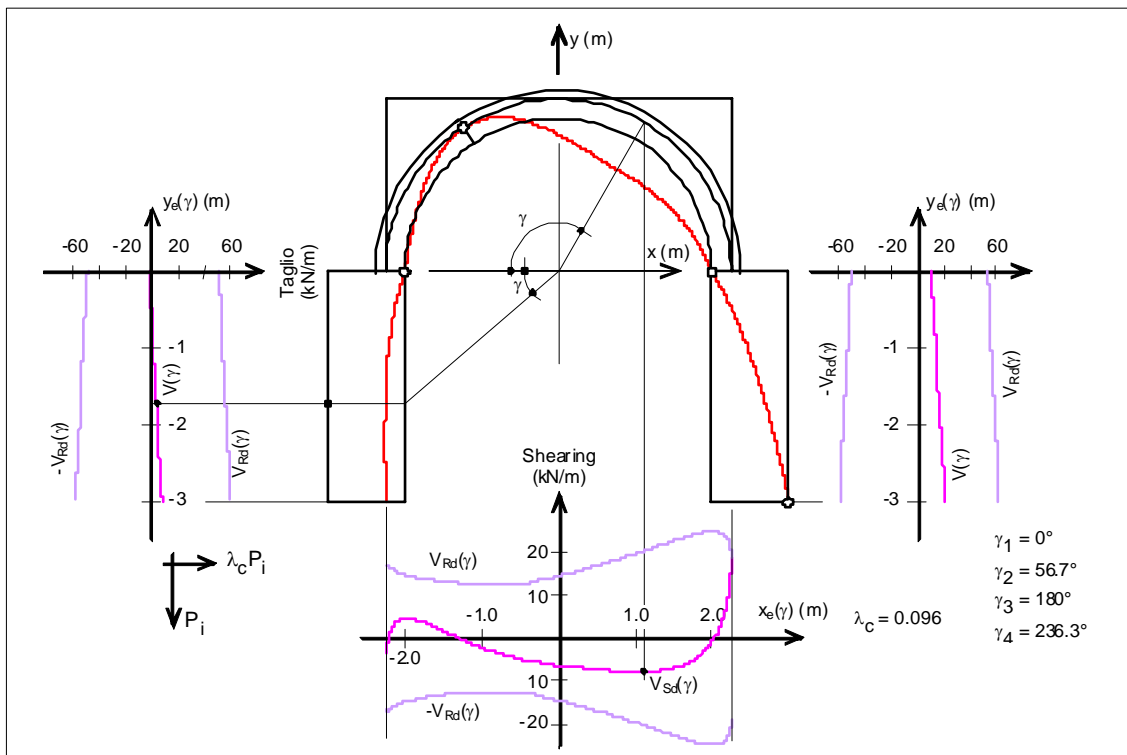


Figure 3.16.



4. PARTITION WALLS

4.1 Aims and criteria of reinforcement with FRCM

Masonry partition walls subject to seismic action may display the typical local mechanisms of collapse shown in the diagram in figure 4.1.

In the context of analysis of the local collapse mechanisms identified in point C8A.4 of [3], spectral acceleration of activation of a collapse mechanism is:

$$a_0^* = \frac{\alpha_0 g}{e^* \cdot FC} \quad (4.1)$$

where e^* is the participating fraction of the mass, calculated as follows:

$$e^* = \frac{gM^*}{P_{tot}} \quad M^* = \frac{1}{g \sum_{i=1}^n P_i \cdot \delta_{xi}^2} \cdot \left(\sum_{i=1}^n P_i \cdot \delta_{xi} \right)^2 \quad (4.2)$$

where M^* is the mass participating in the mechanism:

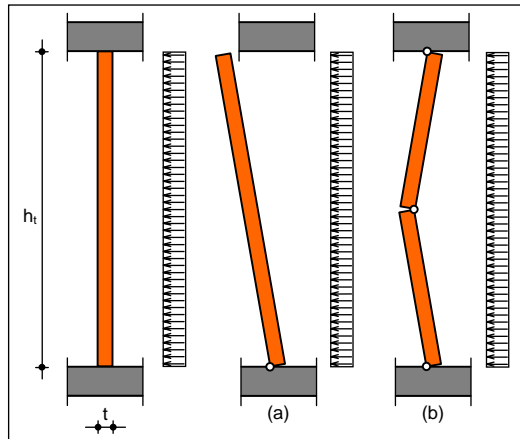


Figure 4.1. Out-of-plane collapse mechanisms in wall partitions.

In (4.1)-(4.3):

α_0 is the horizontal multiplier of activation of the mechanism (figure 15), to be determined by imposing the maximum equilibrium conditions on the system;

g is the acceleration of gravity;

FC is the Confidence Factor, assumed to be 1.35 if the masonry's compression strength is considered to be infinite;

P_{tot} is the total weight of the masses involved in the mechanism;

P_i is the weight of the i -th mass involved in the mechanism, $i = 1, 2, \dots, n$;

δ_{xi} is the virtual horizontal shift in the point of application of the weight P_i , $i = 1, 2, \dots, n$.

In the case of the collapse mechanisms shown in figure 4.1, the system's equilibrium supplies the multipliers:

$$\alpha_0 = \frac{t}{h_t} \quad \text{for the mechanism in figure 4.1 (a);}$$

$$\alpha_0 = 4 \frac{t}{h_t} \quad \text{for the mechanism in figure 4.1 (b);}$$
(4.3)

If the blocks making up the mechanism are not resting on the ground, verification of the Limit State for the Safeguarding of Life is satisfied if the spectral acceleration of activation a_0^* satisfies:

$$a_0^* \geq a_D^* \quad (4.4)$$

where:



$$a_D^* = \frac{S_e(T_1) \cdot \psi(Z) \cdot \gamma}{g} \quad (4.5)$$

with:

$S_e(T_1)$: ordinate of the spectrum of elastic response in relation to the probability of exceeding the reference period V_R , corresponding to period T_1 , by 10%;

T_1 : first natural period of the entire structure;

and as:

$$\psi(Z) = \frac{Z}{H} \quad \gamma = \frac{3N}{2N+1} \quad (4.6)$$

where:

Z: is height, with respect to the foundation of the centre of gravity of the constraints between the blocks involved in the mechanism;

H: is the structure's height above the foundation;

N: is the number of floors in the building.

If condition (5) is not met, it is possible to intervene with FRCM and connectors to reinforce the partition wall.

4.1.1 Design of reinforcement

To prevent the mechanism illustrated in figure 4.1 (a) with a spectral acceleration of a_D^* , we need a reaction binding the upper end of the partition wall equal to:

$$R = \frac{a_D^* \cdot p \cdot h_t}{g \cdot 2} \quad (4.7)$$

To prevent the mechanism illustrated in figure 4.1 (b) with a spectral acceleration of a_D^* we must arrange the composite reinforcement on the surface of the partition wall, designed in order to make sure that the mid-section has a calculated moment of resistance of more than:

$$M_{Sd} = \frac{a_D^* \cdot p \cdot h_t^2}{g \cdot 8} \quad (4.8)$$

The moment of resistance of the reinforced section may be estimated as:

$$M_{Rd} = 0.9 \cdot t \cdot E_f A_f \cdot \varepsilon_{fd} \quad (4.9)$$

where t is the thickness of the partition wall, E_f the modulus of elasticity, A_f the area of the section and ε_{fd} the calculated dilatation of the reinforcement (linked with the phenomenon of delamination). Comparison of (4.8) with (4.9) gives us the necessary reinforcement section:

$$A_f \geq \frac{M_{Sd}}{0.9 \cdot t \cdot E_f \cdot \varepsilon_{fd}} \quad (4.10)$$

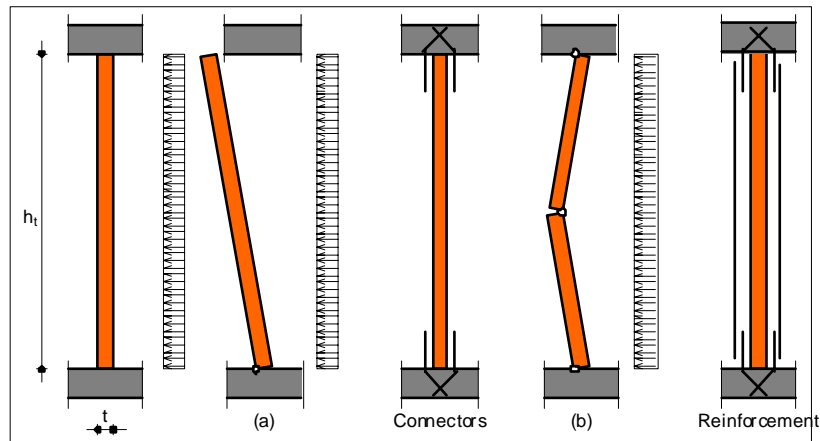


Figure 4.2. Reinforcement with FRCM to prevent out-of-plane collapse mechanisms.

We may conduct a more detailed investigation on the basis of the guidelines [1]. The moment of resistance of the reinforced section may be estimated taking into consideration a “stress-block” approach for the masonry with a compression tension of $0.85 f_{md}$ extended over the section with a depth of $0.8 x$, where f_{md} is the masonry’s calculated compression strength and x is the distance of the neutral axis from the compressed edge (figure 4.3).

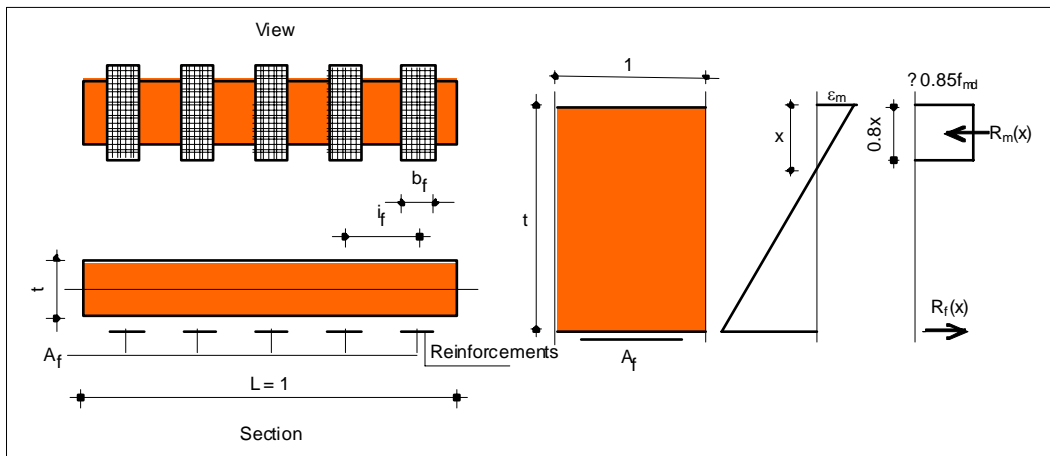


Figure 4.3. Tensions on the section.

In the absence of normal force, the calculated moment of resistance is therefore:

$$M_{Rd} = \varepsilon_f \cdot E_f A_f \cdot (t - 0.4 \cdot x) \quad (4.11)$$

where x is the distance of the neutral axis from the compressed edge, calculated as follows:

$$0.8 \cdot 0.85 \cdot f_{md} \cdot x = \frac{\varepsilon_{mu}}{x} \cdot (t - x) \cdot E_f A_f \quad \text{in the case of breakage when the masonry reaches its ultimate deformation point}$$

$$0.8 \cdot 0.85 \cdot f_{md} \cdot x = \varepsilon_{fd} \cdot E_f A_f \quad \text{in the case of breakage when the reinforcement reaches its calculated ultimate dilation} \quad (4.12)$$

4.1.1.1 Examples

Example 1. Reinforcement of a partition wall against out-of-plane seismic action.

Let us consider the partition wall shown in figure 4.4, consisting of masonry with a calculated compression strength of $f_{md} = 0.5$ MPa. We determine the acceleration of activation of the mechanisms in figure 4.2 and determine the amount of reinforcement with FRCM Ruredil XmeshC10/M25 required to increase it. We consider the response spectrum for the Limit State for the Safeguarding of Life shown in figure 4.4.

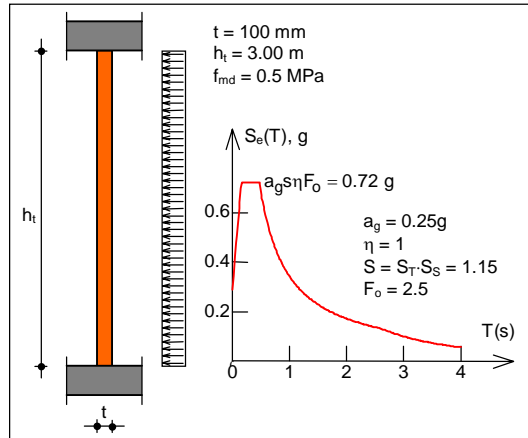


Figure 4.4. Partition wall subject to seismic actions at right angles to the plane.

The system's equilibrium in relation to the collapse mechanism illustrated in figure 4.2 (a) provides us with the horizontal multiplier of activation:

$$\alpha_0 = \frac{t}{h_t} = 0.033$$

and therefore the mechanism's spectral acceleration:

$$a_0^* = \frac{\alpha_0 g}{e^* \cdot FC} = \frac{0.033g}{1 \cdot 1.35} = 0.025 \text{ g}$$

as, for the mechanism under consideration, $e^* = 1$, and taking into account a confidence factor of $FC = 1.35$, as required by [3].

Demand, represented by a_D^* , is:

$$a_D^* = \frac{S_e(T_1) \cdot \psi(Z) \cdot \gamma}{q} = \frac{0.72 \cdot 0.83 \cdot 1.33}{2} \text{ g} = 0.4 \text{ g}$$

taking into consideration the maximum ordinate of the spectrum and $Z = 10 \text{ m}$, $H = 12 \text{ m}$ and $N = 4$ in (7).

The strength of the connectors required to prevent this mechanism is:

$$R = \frac{a_D^* \cdot p}{g} \cdot \frac{h_t}{2} = 0.4 \cdot 1.1 \cdot \frac{3}{2} = 0.66 \frac{\text{kN}}{\text{m}}$$

Considering application of Ruredil XJoint connectors with a diameter of $\phi_c = 12 \text{ mm}$, with an estimated fiber section of:

$$A_{fc} = \frac{1}{3} \cdot \frac{\pi \phi_c^2}{4} = 37.7 \text{ mm}^2$$

and a calculated connector dilation of $\varepsilon_{fcon} = 1\text{‰}$, strength will be:

$$F_{conn} = \frac{A_{fc} \cdot \varepsilon_{fcon} \cdot E_f}{l_{conn}} = 9 \frac{\text{kN}}{\text{m}}$$

The system's equilibrium in relation to the collapse mechanism illustrated in figure 4.2 (b) gives us the horizontal activation multiplier:

$$\alpha_0 = 4 \frac{t}{h_t} = 0.13$$

and therefore a spectral acceleration of mechanism activation of:



$$a_0^* = \frac{\alpha_0 g}{e^* \cdot FC} = \frac{0.13 \cdot g}{1 \cdot 1.35} = 0.096 \text{ g}$$

as, for the mechanism taken into consideration, $e^* = 1$ and we have considered $FC = 1.35$.

Demand, represented by a_D^* , is once again:

$$a_D^* = \frac{S_e(T_1) \cdot \psi(Z) \cdot \gamma}{q} = \frac{0.72 \cdot 0.83 \cdot 1.33}{2} g = 0.4 \text{ g}$$

The moment of resistance required to meet this demand is:

$$M_{Sd} = \frac{a_D^* \cdot p}{g} \cdot \frac{h_t^2}{8} = \frac{0.4 \cdot g \cdot 1.1}{g} \cdot \frac{3^2}{8} = 0.495 \frac{\text{kNm}}{\text{m}}$$

Considering that Ruredil XMesh C10/M25 reinforcement has a calculated reinforcement dilation of $\varepsilon_{fd} = 3\text{‰}$, the reinforcement section required is approximately:

$$A_{f \min} = \frac{M_{Sd}}{0.9 \cdot t \cdot E_f \cdot \varepsilon_{fd}} = 7.76 \frac{\text{mm}^2}{\text{m}}$$

If we apply vertical strips 330 mm wide with a centre-to-centre distance of 1 m (figure 4.5), the reinforcement section will be:

$$A_f = 0.047 \frac{330}{1000} = 15.51 \frac{\text{mm}^2}{\text{m}}$$

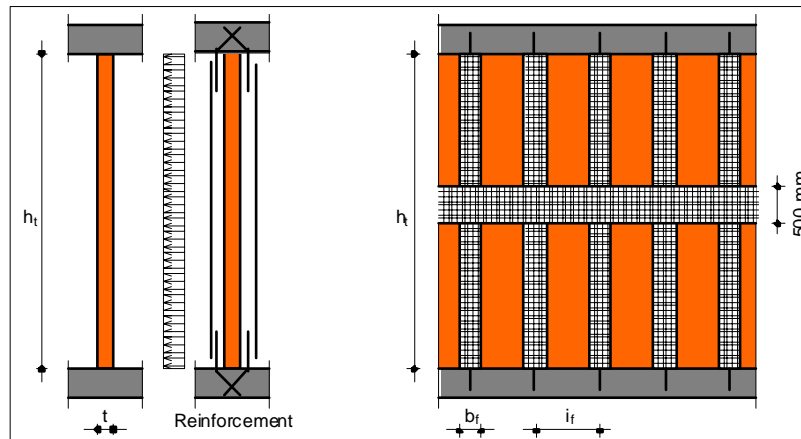


Figure 4.5. Reinforcement configuration of a partition wall with FRCM.

With this reinforcement configuration, supposing that breakage is on the tensile side (reaching ε_{fd} in the fibers), the distance of the neutral axis from the compressed edge will be:

$$x = \frac{\varepsilon_{fd} \cdot E_f A_f}{0.8 \cdot 0.85 \cdot f_{md}} = \frac{3 \cdot 240000}{1000 \cdot 0.8 \cdot 0.85 \cdot 0.5} \cdot \frac{15.51}{1000} = 32.8 \text{ mm}$$

and the maximum deformation of the masonry will be:

$$\varepsilon_m = \varepsilon_f \cdot \frac{x}{t - x} = 1.47 \text{ ‰}$$

This value confirms the assumption of breakage in the tensile area.

Finally, the section's calculated moment of resistance will be:

$$M_{Rd} = \varepsilon_{fd} \cdot E_f A_f \cdot (t - 0.4 \cdot x) = \frac{3}{1000} \cdot 240 \cdot 15.51 \cdot (0.1 - 0.4 \cdot 0.0328) = 0.97 \frac{\text{kNm}}{\text{m}}$$

For better division of stresses, the diagram in figure 4.5 also considers a horizontal reinforcement 500 mm wide.



References

- [1] CNR DT200/2004 Instructions for the Design, Execution and Control of Static Consolidation Work using Fiber Reinforced Composites, 2004.
- [2] January 14 2008 Ministerial Decree. Technical regulations for construction.
- [3] February 2 2009 memorandum no. 617. Instructions for application of the technical standards for constructions contained in the January 14 2008 ministerial decree.

Basic bibliography

Compositi a matrice cementizia per il rinforzo di volte in muratura [F. Focacci, G. Mantegazza, Study day on "Monumental restoration in the Egadi Islands", Palazzo Florio, Favignana, October 12 2007]

FRCM vs. FRP composite to strengthen RC beams: a comparative analysis [a. Di Tommaso, F. Focacci, G. Mantegazza, A. Gatti, FRPRCS-8 University of Patras, Patras, Greece, July 16-18, 2007]

How durable is FRP-plated concrete under moisture? [O. Buyukozturk, FRPRCS-8 University of Patras, Patras, Greece, July 16-18, 2007]

Externally bonded FRP reinforcement for RC structures [FIB Bulletins n. 14]

FRP reinforcement in RC structures [FIB Bulletins n. 40]

Guide for the Design and Construction of Externally Bonded FRP Systems for Strengthening Concrete Structures. [ACI 440.2R]

Istruzioni per la progettazione di interventi di consolidamento statico mediante l'utilizzo di compositi fibrorinforzati a matrice cementizia FRCM

(Instructions for planning static consolidation projects using fiber reinforced cementitious matrix compounds)